INCORPORATION OF DSSC IN REAL TIME CONGESTION MANAGEMENT


A THESIS SUBMITTED TO
THE GRADUATE SCHOOL OF NATURAL AND APPLIED SCIENCES
OF
MIDDLE EAST TECHNICAL UNIVERSITY


BY

RAMAZAN GÜNAY


IN PARTIAL FULLFILMENT OF THE REQUIREMENTS
FOR
THE DEGREE OF MASTER OF SCIENCE
IN
ELECTRICAL AND ELECTRONICS ENGINEERING


JANUARY 2018

Approval of the thesis:

**INCORPORATION OF DSSC IN REAL TIME CONGESTION MANAGEMENT**

submitted by **RAMAZAN GÜNAY** in partial fulfillment of the requirements for the degree of **Master of Science in Electrical and Electronics Engineering Department, Middle East Technical University** by,

Prof. Dr. Gülbin Dural Ünver       _____
Dean, Graduate School of **Natural and Applied Sciences**

Prof. Dr. Tolga Çiloğlu       _____
Head of Department, **Electrical and Electronics Engineering**

Assist. Prof. Dr. Murat Göl       _____
Supervisor, **Electrical and Electronics Eng. Dept., METU**

**Examining Committee Members:**

Prof. Dr.  Ali Nezih Güven       _____
Electrical and Electronics Engineering Dept., METU

Assist. Prof. Dr. Murat Göl       _____
Electrical and Electronics Engineering Dept., METU

Assist. Prof. Dr. Ozan Keysan       _____
Electrical and Electronics Engineering Dept., METU

Assist. Prof. Dr. Ayşe Selin Kocaman       _____
Industrial Engineering Dept., Bilkent University

Assist. Prof. Dr. Oğuzhan Ceylan       _____
Management Information Systems Dept., Kadir Has University

**Date:**    **19.01.2018**

I hereby declare that all information in this document has been obtained and presented in accordance with academic rules and ethical conduct. I also declare that, as required by these rules and conduct, I have fully cited and referenced all material and results that are not original to this work.

Name, Last name : Ramazan Günay

Signature             :

# ABSTRACT

## INCORPORATION OF DSSC IN REAL TIME CONGESTION MANAGEMENT

Günay, Ramazan

MS., Department of Electrical and Electrons Engineering

Supervisor     : Assist. Prof. Dr. Murat Göl

January 2018, 79 pages

Congestion became an inseparable part of power system operation, after deregulation of the monopolistic electric market. Presence of congestion causes rise of local market powers, and hence it is avoided during day-ahead planning. However, it is possible to encounter congestion during real-time operation because of the uncertain behavior of the loads. Although, the congestion can be detected in real-time, its management is not trivial as it requires change of topology or generation dispatch.

This work proposes a real-time congestion management method with the help of Distributed Static Series Compensators (DSSCs). DSSC is a Flexible AC Transmission System (FACTS), which can alter the series impedance of transmission line it is connected, and communicate between each other and a master controller. Although number of installed DSSCs is very low for the time-being, it is expected

that DSSCs will be populate rapidly for power flow control thanks to its high reliability, fast response time and low cost advantages.

This thesis firstly introduces a method for optimal placement of DSSCs to obtain system controllability. Then an algorithm is developed to control the considered power system with DSSCs in real time. The algorithm aims to control power flow to avoid congestions and to minimize system losses. The proposed methods are validated using numerical examples.

# ÖZ

## GERÇEK ZAMANLI HAT TIKANIKLIKLARININ GİDERİLMESİNDE DSSC KULLANIMI

Günay, Ramazan

Yüksek Lisans, Elektrik Elektronik Mühendisliği Bölümü

Tez Yöneticisi: Yrd. Doç. Dr. Murat Göl

Ocak 2018, 79 sayfa

Hatlardaki tıkanıklıklar, monopol elektrik piyasasının özelleştirilmesinin ardından elektrik şebekesinin ayrılmaz bir parçası haline gelmiştir. Bu tıkanıklıklar bölgesel piyasa etkilerini artırmaktadır, bu nedenle gün öncesi planlamada tıkanıklıklar engellenmeye çalışılmaktadır. Bununla birlikte, gün içerisinde, yüklerin belirsiz karakterlerinden dolayı tıkanıklık olma ihtimali yine de vardır. Hat tıkanıklıkları gerçek zamanlı olarak tespit edilebiliyor olsa da, topoloji veya jeneratörlerin güçlerinin yeniden düzenlenmesini gerektirdiği için yönetilmesi kolay değildir.

Bu çalışmada dağıtılmış statik seri kompansatörler (DSSC) kullanılarak gerçek zamanlı tıkanıklıkların yönetilmesi amaçlanmaktadır. DSSC esnek AC iletim sistemi (FACTS)'nin bir türüdür. Bağlandıkları iletim hatlarının seri empedansını değiştirirler ve kendi aralarında veya merkezi bir kontrolörle haberleşebilirler. Mevcut durumda DSSC cihazları çok fazla kullanılmamaktadır, ancak yüksek

güvenilirlik, hızlı tepki süresi ve düşük maliyet avantajları sayesinde güç akışı kontrolü için gelecekte çokça kullanılacakları düşünülmektedir.

Bu tez, ilk olarak sistemi kontrol edilebilir hale getirmek için DSSC'lerin optimum yerleştirilmelerinden bahsetmektedir. Daha sonra, söz konusu şebekeyi kontrol etmek için bir algoritma geliştirilmiştir. Bu algoritma, tıkanıklıkları önlemek amacıyla hatlardaki güç akışlarını kontrol etmeyi ve sistem kayıplarını düşürmeyi amaçlamaktadır. Önerilen yöntemler numerik örneklerle ispatlanmıştır.

Anahtar Kelimeler: Dağıtılmış Statik Seri Kompansatör, Kontrol edilebilirlik, Güç Akış Kontrolü, Kayıpların Düşürülmesi, Hat Tıkanıklıklarının Yönetilmesi

# ACKNOWLEDGEMENTS

# TABLE OF CONTENTS

# LIST OF TABLES

# LIST OF FIGURES

FIGURES

# CHAPTER 1

## INTRODUCTION

Power flow control is one of the most important problems of power system, especially after the deregulation of the electric power market. Uncontrolled power flow may cause congestions in the system, which may affect the market and result in arise of local market powers. Moreover, line congestions hinder some of the bilateral agreements and complete utilization of the available system. Due to the congestions, economic dispatch of the generators cannot be achieved, and that gives rise to increase of electrical prices. This phenomenon is called the congestion cost. For instance, over 50 transmission corridors in the U.S. are routinely congested, resulting in high economic burden [1], for example according to the New York Independent System Operator (NYISO), transmission and distribution system congestion cost is over U.S.$ 1 billion per year [2]. Constructing new transmission lines may solve the problem, but construction cost is very high and requires several years, which means the continuation of the congestion problem for additional couple of years. Power flow control is the most beneficial way to relieve the lines, which also provides some additional benefits to the system such as;

- Relieve overloaded lines
- Reduce transmission losses
- Maintain acceptable voltages
- Improve voltage and transient stability

The active power flow through a transmission line can be expressed as shown in (1) in a simplified manner. Considering (1), one should manipulate the sending and

receiving end bus voltage magnitudes ($|V_i|$, $|V_j|$), difference between the sending and receiving end voltage phase angles ($\delta$) or line impedance ($x_{ij}$), to control the active power flow.

$$P_{ij} = \frac{|V_i||V_j|}{x_{ij}}\sin(\delta) \tag{1}$$

As voltage magnitudes and phase angles are determine based on the operating conditions and the parameters of the considered system, most of the power flow control devices change the effective impedance of the line for power flow control. Impedance change can be achieved either via physical components, such as capacitors and inductors (passive impedance injection), or by power electronics based devices such as Flexible AC Transmission System (FACTS) and distributed-FACTS (DFATCS) (active impedance injection).

Passive impedance injection is the cheapest solution for power flow control. Despite the low price and ease of application, those systems have some drawbacks. As it can be seen from Figure 1, they are established on the ground and hence require HV insulation, which reduces the reliability. Besides, series capacitors may lead to sub-synchronous resonance [3]. Moreover, connected passive elements need reactive power for their operation, and hence all of the supplied energy cannot be transferred to the load. Last but not the least, passive impedance injection cannot provide dynamic support, such that real time control of the power flow cannot be achieved. For instance on 31 March 2015, an unexpected relay operation and some other unexpected mishaps led to a blackout in Turkey which costs about 1 billion dollars. There were series capacitors on those lines to control power flow, but those capacitors were out of service for maintenance. If controllable active devices were used instead of series capacitors, blackout might have been prevented via power flow control. Considering those disadvantages, active impedance injection may be a better choice for real time power flow control and congestion management.

2

*Figure 1 Series Capacitors [4]*

FACTS devices are power electronic based devices with high rated power, which can be employed for power flow control. FACTS devices have series, shunt, and series and shunt types. They can control P, Q, or both P and Q of the considered line. Figure 2 shows a sample implementation of FACTS devices. Types of FACTS devices can be listed as follows [5]:

- Static VAR Compensator (SVC): SVC is a thyristor–controlled shunt device, which may utilize capacitors or reactors. It can improve system stability and provide voltage control.

- Thyristor–Switched Series Capacitors (TSSC): TSSC is thyristor – controlled capacitor. It can provide both capacitive and inductive support.

- Static Synchronous Series Compensators (SSSC): SSSC uses a synchronous voltage source (SVS) to inject reactive power to the line. It can provide both capacitive and inductive support. Thus, it can both increase and decrease the real power flow of the line.

- Static Synchronous Condensers (STATCOM): STATCOM uses a synchronous voltage source (SVS) to inject reactive power to the line. It

provides reactive power to the system and works as a synchronous condenser.

- Unified Power Flow Controller (UPFC): UPFC is a combination of SSSC and STATCOM. It can provide both series and shunt compensation. Hence, it can control voltages, real and reactive power flows at the same time.



*Figure 2 FACTS Installation at field [6]*

Although FACTS devices are in the market to control power flow for about 20 years, wide deployment could not be achieved due to some barriers, which can be listed as below [7].

- High investment cost: FACTS devices are power electronics devices with high rated power; therefore component and device development costs are high.

- Low reliability: FACTS devices need to be installed on the ground; therefore they need high voltage insulation, which reduces the reliability.

- High initial cost: Since FACTS devices are not modular, initial cost is high, and this leads to low rate of return.

- Maintenance requirements: Due to their complex structure and high voltage insulation requirements, FACTS devices require on-site repair.

- High operation cost: Custom-engineered system increases the operation cost.

DFACTS devices, which are introduced recently, have the potential to remove the barriers of FACTS devices. They have high reliability compared to the conventional solutions, since they do not need HV insulation as they are directly clamped to the transmission lines. Moreover, DFACTS cost is much less than FACTS devices, such that cost of FACTS is 120-150 $/kVAr while cost of DFACTS is 100 $/kVA [1]. For a 30-year of usage, it is estimated that total cost of DFACTS should be less than half of the FACTS devices' cost [1]. Although passive impedance injection is a much cheaper solution compared to the both static solution, the fact that passive impedance injection can either reduce or increase the power flow while DFACTS can be used to both increase and decrease the power flow, makes DFACTS more favorable in real time power flow control. Moreover, DFACTS does not cause sub-synchronous resonance, which is considered as another advantage.

DFACTS devices have two types, such that they can be connected to the system either in series or shunt. Series DFACTS devices can be used to control active power flow, whereas shunt devices can be used to regulate voltage magnitudes. Therefore, thesis considers series DFACTS to control the power flow on transmission lines. The series DFACTS can be further classified into two classes [8]. Those are Distributed Series Reactor (DSR) and Distributed Static Series Compensator (DSSC) devices. DSR devices can only increase the line impedance by inductive voltage injection [9], while DSSC can both increase and decrease the line flow. In this study, we used DSSC devices for real time control of the system, because of its capability of both increasing and decreasing the line power flow. Figure 3 shows a DSSC implementation.

*Figure 3 Installed DSSC [10]*

There are only a few studies on capability of DSSC devices regarding the power flow control. In [7] and [11], it is proven that DSSC devices can be used for power flow control, loss minimization and voltage control. In those studies, the researchers try to control power flow of a specific single line with DSSC devices. In the literature, there is not any study aiming to control whole power system in real time, to avoid congestion. This thesis aims to control the power flows of all lines in real time with simultaneous use of DSSC, in order to make the system operate with minimum loss and without any congestion.

The thesis is organized as follows. In Chapter 2 a detailed review of DSSCs is provided. Chapter 3 utilizes the simplified power flow to impedance sensitivity matrix, in order to place DSSCs optimally for system controllability. Chapter 4 develops the central power flow control method to avoid congestion in real time. Finally Chapter 5 validates the proposed method, followed by conclusions in Chapter 6.

# CHAPTER 2

# DSSC DEVICES

This chapter introduces Distributed Static Series Compensator Devices (DSSC) devices. Firstly, the operation principle is explained in detail, followed by the determination of the relation between injected impedance and line current. Then, potential applications of DSSC devices are explained.

## 2.1 Device Structure and Operation Principle

DSSC is a type of DFACTS, which can change the effective impedance of the line by voltage injection using a synchronous voltage source (SVS) [12]. SVS generates sinusoidal voltages at fundamental frequency, i.e. 50 or 60 Hz, with controllable amplitude and phase angle [13]. Voltage that is in quadrature with the line current is injected to the connected transmission line via the single turn transformer (STT), which has a transmission conductor as secondary winding and injects the desired voltage in the cable itself [14]. Figure 4 shows schematic diagram of the DSSC.

DSSCs can only be activated if the line current is higher than a threshold value. If the line current is less than the threshold value, STT is bypassed, otherwise, DSSC is activated, and injects desired voltage to the line. Note that, the line is an inductive current source for STT.
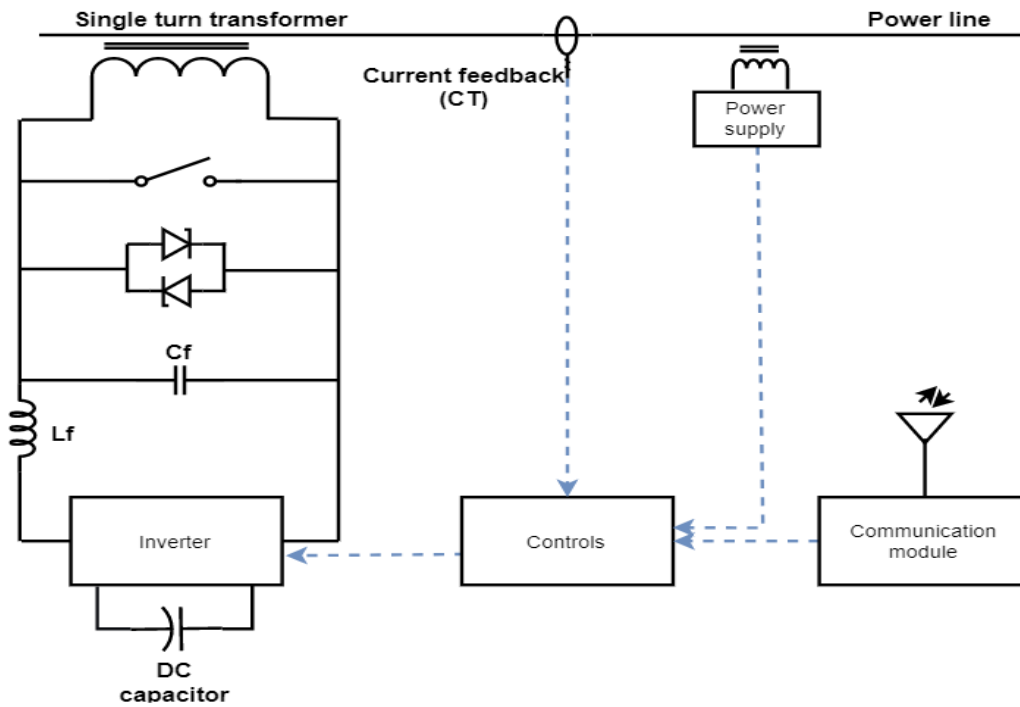
*Figure 4 DSSC Circuit*

The injected voltage to the line is controlled using pulse width modulation (PWM) methods. Voltage magnitude and phase angle are adjusted by the inverter, which has four switching devices, a filter and a DC-link capacitor. Although DSSC devices provide reactive power compensation to the line, a small amount of real power is absorbed from the line due to the losses of DSSC, therefore phase angle difference between the injected voltage and line current is a little bit less than 90 degree.

Depending on the injected voltage, power flow of the considered line can be both increased and decreased, such that If the injected voltage lags line current, device works capacitive, therwise the device works inductive.

DSSC devices can either be controlled from a controller center using power line communication method or wireless communication, or work autonomously. Figure 5 shows the how the injected voltage by the DSSCs affects the line as a reactance ($X_{DSSC}$).
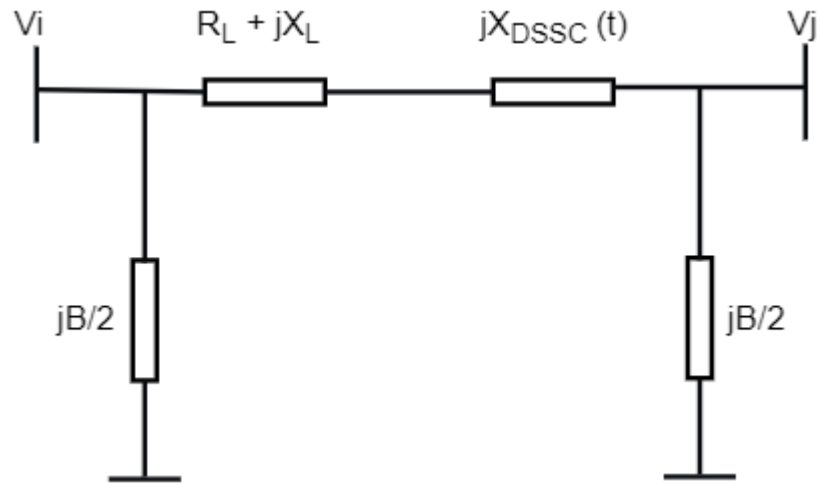
*Figure 5 Impedance Injection Using DSSC*

DSSC devices are single phase and relatively small devices, typically ranging between 10-20 kVA, and 45-75 kg. Therefore, to accomplish a certain function on a transmission line, a great number of devices are required to be installed and controlled at the same time. All devices has a communication module, and they can communicate with each other and a central controller to realize a function like power flow control, loss minimization or power quality improvement.

DSSC devices' effect on line impedance depends on the magnitude of the line current. Injected impedance reduces as the line current increases as seen in Figure 6. This relation is formulized in (2), where $X_{inj}$ is the effective impedance injected to the line, and $Q_{inj}$ is the reactive power injected by the DSSC.

$$X_{inj} = \frac{Q_{inj}}{I_{line}^2} \tag{2}$$
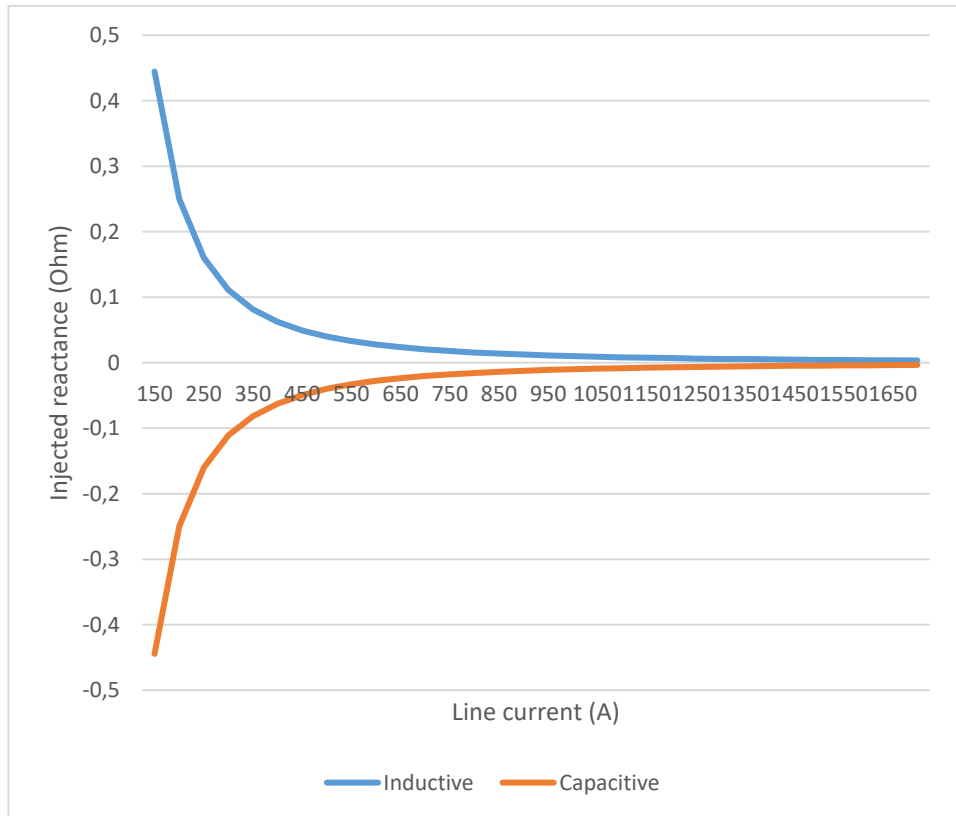
*Figure 6 Effective Impedance for a DSSC Model with 10 kVA, 6 V RMS Output Capability at 1700 A RMS*

STT is a very important component for DSSC devices. It enables DSSC to clamp on the line. Turns ratio of STT is very high, which decreases the current flow through the inverter of DSSC. Even during a fault, current flow through the DSSC is less than the 700 A, which can be handled easily. DSSC devices can also change the line impedance within milliseconds to control the current.

The DSSC devices to be clamped on the lines should meet the capability of injecting sufficient reactance in accordance with the line fault current. The devices should be specified properly by considering line current flows through a targeted transmission line in both normal and emergency states [15]. Minimum and maximum operation current and voltage must be defined properly; otherwise desired control may not be achieved.

10

## 2.2 Relationship between Injected Voltage and Real Power Flow

Although voltage injection is can be modeled, as change of line impedance, actual effect of voltage injection is a little bit different. Relationship between the line impedances and power flow is defined as follows [1]. In (3), Vq is injected voltage to the line.

$$P_{ij} = \frac{V_i V_j \sin\delta}{X} - \frac{V_i V_q \cos(\frac{\delta}{2})}{X} \left[ \frac{\sin(\frac{\delta}{2})}{\sqrt{\left(\frac{V_i+V_j}{2V_j}\right)^2 - \frac{V_i \cos^2(\frac{\delta}{2})}{V_j}}} \right] \tag{3}$$

Despite the relation between the injected voltage and line active power flow is well defined as seen in (3), it is easier to model the effect of DSSC as an impedance injection as shown in Figure 5.

Figure 7 and 8 show relation between transmitted power on the line and impedance injection and voltage injection, respectively. As it can be seen from Figure 8, negative voltage injection creates capacitive effect, and increases the power flow of the line.
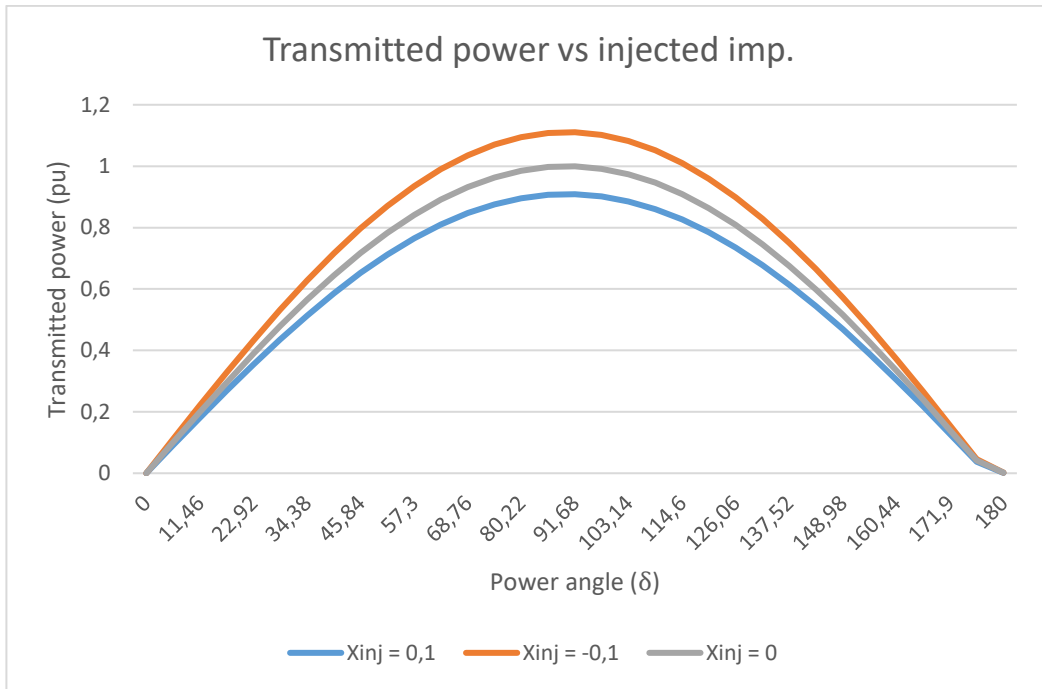
*Figure 7 Effect of Impedance Injectıon on Line Real Power Flow*



*Figure 8 Effect of Voltage Injection on Line Real Power Flow*

## 2.3 Potential Applications of DSSC

DSSC devices can be used to control power flow, reduce system losses, increase system stability and facilitate renewable integration. Moreover, DSSC technology can suppress effectively voltage fluctuation, voltage flicker, voltage sag and interruption, reduce harmonics and distortion, and eliminate unbalance of three phase voltage [16]. However, since DSSC devices provide series compensation, bus voltage magnitudes cannot be controlled effectively using DSSC devices.
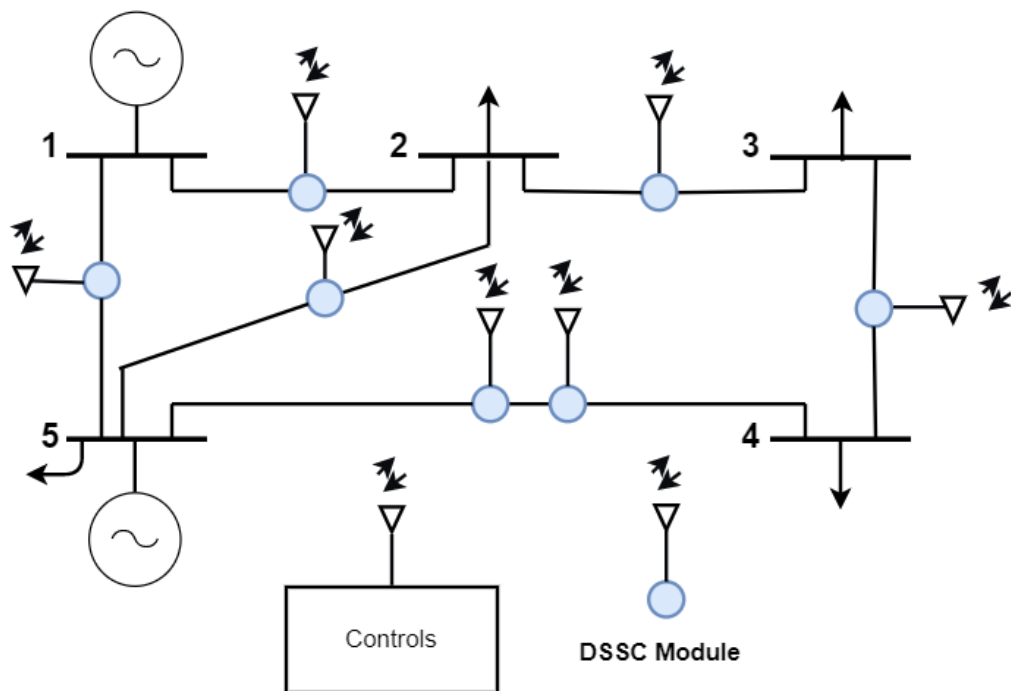


*Figure 9 DSSC Implementation*

In the Figure 9, a sample implementation of DSSC devices is shown. DSSC devices can either be placed on certain lines or all of the lines. To be able to provide a robust coordination among the DSSC devices, mishaps such as communication line outage, fault, and contingency must be considered. By defining the impedance injections as a function of line currents, whole system can be effectively controlled. For instance,

if the line is 90% loaded, line impedance can be increased gradually to reduce the line current.

DSSC devices can be coordinated to accomplish certain functions. Those functions are listed below:

- Loss minimization.
- Redistribution of line current in case of an line outage.
- Eliminating the sub synchronous resonance (SSR).
- In case of a contingency, increasing the line currents above their thermal limits.
- Reduction of oscillations.
- Increasing the ATC by controlling the power flows of flow-gates.
- Reduction of line currents.
- Congestion management.

DSSC devices provide distributed solution to power flow control problem, such that many number of devices are used rather than a bulk system to control a certain amount of power. Therefore, as the system capacity rises, additional DSSC devices can be added to the system. Number of DSSC devices can be determined by calculating the annual necessary additional available transfer capacity (ATC).

*Table 1 Calculation of Number of DSSC Modules to Change Line Impedance by 1%*

| Line voltage | 138 kV | 345 kV | 765 kV |
|---|---|---|---|
| Line capacity | 180 MVA | 1200 MVA | 6600 MVA |
| Reactance (Ohm/km) | 0.78 | 0.60 | 0.54 |
| Voltage drop/km | 608 V | 1200 V | 2700 V |
| 1% compensation /km | 6 V | 12 V | 27 V |
| DSSC kVA/km | 14 kVA | 72 kVA | 400 kVA |
| Total 10 kVA DSSC devices/km/ | 1.4 | 7.2 | 40 |

Table 1 shows the typical characteristics of 138, 345 and 765 kV lines and necessary number of DSSC devices for those lines to change the line impedance 1%. Line characteristics are representative. For instance for the 345 kV line, voltage reduction is 1200 V/km under the rated line current. Thus, to be able to change line impedance 1%, 12 V/km voltage must be injected to the line. This can be achieved by using 72 kVA/km DSSC devices. To change the line impedance 20%, 1440 kVA /km compensation is necessary. This compensation can be achieved using 144 DSSC devices. That means 48 DSSC device/phase/km is necessary.

Distributed nature of DSSC devices provides some advantages. One of the most important advantages is, the installation cost is decreased by spreading the investment cost to a wide time interval [1]. For instance, FACTS devices are designed considering the long term demand. Thus, only a small portion of the total capacity may be used during the first years. On the other hand, DSSC devices can be placed only considering the current demand, and as demand increases, number of devices can be increased gradually. Long term estimations can also be misleading, and installed capacity may be more than the total demand. This leads to poor return on investment.

DSSC devices bring some operational and economic advantages, as well. Those advantages are listed as follows.
- Line current can be adjusted according to the line temperature.
- Reliability and redundancy is very high.
- Device installation is very easy.
- Line current can be increased and decreased.
- DSSC devices can be used for different types of conductors.
- Operation cost of the system can be decreased by decreasing the losses.
- Asset utilization can be increased.
- Available transfer capacity (ATC) can be increased.
- New line requirement can be reduced.

- Congestion management can be achieved.
- Bilateral agreements can be completed and cost of electricity can be decreased.
- Initial cost can be decreased.

## 2.4 Conclusion

DSSC is a power flow control device that provides its energy demand from lines without requirement of HV insulation, and can be controlled remotely by means of the communication module. To be able to achieve a certain function, great number of DSSC devices must be controlled simultaneously. DSSC devices can both increase and decrease the line impedance. Thus, they can control the line current. DSSC devices provide distributed solution, they have potential to remove the barriers of lumped power flow control devices such as FACTS, capacitors and phase shift transformers. Large – scale power flow control may finally be achievable via DSSCs.

# CHAPTER 3

## OPTIMAL PLACEMENT OF DSSCS FOR SYSTEM CONTROLLABILITY

In this chapter, a method to optimally place DSSC devices for system controllability is described. In order to achieve this goal, relationship between the line impedances and real power flows of the lines are considered using coupling index.

DSSC devices must be optimally located to the lines so that all the lines can be controlled using minimum number of devices. To control the whole system using DSSC devices, which change the effective line impedance, relationship between the line impedances and real power flows must be known. This relationship can either be calculated via dynamic equations of the system, or using linearized equations of the system under steady state. According to the control theory, controllability is ability to transfer a system from an initial state to a desired final state in a finite time; therefore, to be able to make a system fully controllable, dynamic behavior of the system must be known. However, obtaining the dynamic equations of whole power system can be tedious. Instead, this study uses power flow to impedance sensitivity matrix as control matrix, and analyzes the system in steady state. Note that, effect of impedance change to the transient stability should be analyzed separately. Once relationship between the line impedances and real power flows are calculated, DSSC devices can be placed to the most effective lines, such that device locations and numbers can be easily determined.

Line impedances affect the real power flows in two manners, which are direct and indirect ways. Impedance change affects the real and imaginary parts of the bus impedance matrix, (G and B, respectively,) of the system, which enables

manipulation of power flows on the lines as it can be seen from (4). This is the direct effect of line impedances on real power flows. On the other hand, impedance change affects system states, and system states affect real power flows. This effect is called indirect effect. To obtain the full relationship between the line impedances and real power flows, both direct and indirect components must be calculated separately. In (4), $G_{ij}$ is real part of $ij^{th}$ entry of the bus impedance matrix and $B_{ij}$ is imaginary part of $ij^{th}$ entry of the bus impedance matrix.

$$P_{ij} = |V_i||V_j|[G_{ij}cos\Theta_{ij} + B_{ij}sin\Theta_{ij}] - G_{ij}|V_i|^2 \tag{4}$$

## 3.1 Power Flow to Impedance Sensitivity Matrix

Power flow to impedance sensitivity, which shows the relationship between line impedances and real power flows can be calculated using the linearized equations. Equation (5) and (6) shows the complete relationship between the real power flows and line impedances and (7) shows relationship between system states and line impedances [11]. In those equations, $[\Sigma]$ is power flow to system states sensitivity matrix, $[\Gamma]$ is power flow to impedance sensitivity matrix and $[\Phi]$ is system states to impedance sensitivity matrix.

$$[\Delta P] = [\Sigma]\begin{bmatrix} \Delta\theta \\ \Delta v \end{bmatrix} + [\Gamma][\Delta x] \tag{5}$$

$$[\Delta P] = ([\Sigma][\Phi] + [\Gamma])[\Delta x] \tag{6}$$

where,

$$\begin{bmatrix} \Delta\theta \\ \Delta v \end{bmatrix} = [\Phi][\Delta x] \tag{7}$$

$$\Phi = -J^{-1}\Upsilon \tag{8}$$

In (8), J is Jacobian matrix of the system that indicates the relationship between real and reactive power injections and system states. $\Upsilon$ is real and reactive power

injection to impedance sensitivity matrix. Elements of $\Sigma$, J, $Y$, $\Gamma$ are calculated using the partial derivatives.

Elements of J matrix can be defined as follows.

$$\frac{\partial \Delta P_i}{\partial \theta_j} = -V_i \sum_{k=1}^{n} |V_k| \left[ G_{ik} sin\theta_{ik} - B_{ij} cos\theta_{ik} \right] \quad i = j \tag{9}$$

$$\frac{\partial \Delta P_i}{\partial \theta_j} = V_i V_j \left[ G_{ij} sin\theta_{ij} - B_{ij} cos\theta_{ij} \right] \quad i \neq j \tag{10}$$

$$\frac{\partial \Delta P_i}{\partial V_j} = 2V_i G_{ii} + \sum_{k=1}^{n} |V_k| \left[ G_{ik} cos\theta_{ik} + B_{ij} sin\theta_{ik} \right] \quad i = j \tag{11}$$

$$\frac{\partial \Delta P_i}{\partial V_j} = V_i \left[ G_{ij} cos\theta_{ij} + B_{ij} sin\theta_{ij} \right] \quad i \neq j \tag{12}$$

$$\frac{\partial \Delta Q_i}{\partial \theta_j} = V_i \sum_{k=1}^{n} |V_k| \left[ G_{ik} cos\theta_{ik} + B_{ik} sin\theta_{ik} \right] \quad i = j \tag{13}$$

$$\frac{\partial \Delta Q_i}{\partial \theta_j} = -V_i V_j \left[ G_{ij} cos\theta_{ij} + B_{ij} sin\theta_{ij} \right] \quad i \neq j \tag{14}$$

$$\frac{\partial \Delta Q_i}{\partial V_j} = -2V_i B_{ii} + \sum_{k=1}^{n} |V_k| \left[ G_{ik} sin\theta_{ik} - B_{ik} cos\theta_{ik} \right] \quad i = j \tag{15}$$

$$\frac{\partial \Delta Q_i}{\partial V_j} = V_i \left[ G_{ij} sin\theta_{ij} - B_{ij} cos\theta_{ij} \right] \quad i \neq j \tag{16}$$

Elements of $Y$ matrix are defined as follows.

$$\frac{\partial P_i}{\partial x_{ij}} = -V_i^2 \left[ \frac{\partial G_{ij}}{\partial x_{ij}} \right] + V_i V_j \left( \left[ \frac{\partial G_{ij}}{\partial x_{ij}} \right] cos\theta_{ij} + \left[ \frac{\partial B_{ij}}{\partial x_{ij}} \right] sin\theta_{ij} \right) \tag{17}$$

$$\frac{\partial Q_i}{\partial x_{ij}} = V_i^2 \left[ \frac{\partial B_{ij}}{\partial x_{ij}} \right] + V_i V_j \left( \left[ \frac{\partial G_{ij}}{\partial x_{ij}} \right] sin\theta_{ij} - \left[ \frac{\partial B_{ij}}{\partial x_{ij}} \right] cos\theta_{ij} \right) \tag{18}$$

Power flows to system states sensitivities can be defined as below.

$$[\Delta P_{ij}] = [\Sigma] \begin{bmatrix} \Delta \theta \\ \Delta v \end{bmatrix} \tag{19}$$

Elements of $\Sigma$ matrix are specified as follows.

$$\frac{\partial P_{ij}}{\partial \theta_i} = -V_i V_j \left[ G_{ij} sin\theta_{ij} + B_{ij} cos\theta_{ij} \right] \tag{20}$$

19

$$\frac{\partial P_{ij}}{\partial \Theta_i} = V_i V_j \left[ G_{ij} sin\Theta_{ij} + B_{ij} cos\Theta_{ij} \right] \quad (21)$$

$$\frac{\partial P_{ij}}{\partial V_i} = -2V_i G_{ii} + V_j \left[ G_{ij} cos\Theta_{ij} + B_{ij} sin\Theta_{ij} \right] \quad (22)$$

$$\frac{\partial P_{ij}}{\partial V_j} = V_i \left[ G_{ij} cos\Theta_{ij} + B_{ij} sin\Theta_{ij} \right] \quad (23)$$

Power flows to impedance sensitivities (direct sensitivities) are formulated below.

$$[\Delta P_{ij}] = [\Gamma][\Delta x] \quad (24)$$

Elements of $\Gamma$ matrix are defined as below.

$$\frac{\partial P_{ij}}{\partial x_{ij}} = -V_i^2 \left[ \frac{\partial G_{ij}}{\partial x_{ij}} \right] + V_i V_j \left( \left[ \frac{\partial G_{ij}}{\partial x_{ij}} \right] cos\Theta_{ij} + \left[ \frac{\partial B_{ij}}{\partial x_{ij}} \right] sin\Theta_{ij} \right) \quad (25)$$

Despite the voltage magnitudes are sensitive to the impedances and they are used for sensitivity calculations, it will be seen later that, DSSC devices affect the bus voltage magnitudes less than 1%. Hence, to reduce the calculation time, the reduced sensitivities are defined, which only considers voltage phase angles as system states during the process. The reduced relations are given below.

$$[\Delta\Theta] = [\Phi_{reduced}][\Delta x] \quad (26)$$

$$[\Delta P_{ij}] = [\Sigma_{reduced}][\Delta\Theta] \quad (27)$$

$$\Phi_{reduced} = -J_{reduced}^{-1}\Upsilon \quad (28)$$

Elements of $J_{reduced}$ matrix are derived as follows.

$$\frac{\partial \Delta P_i}{\partial \Theta_j} = -V_i \sum_{k=1}^{n} |V_k| \left[ G_{ik} sin\Theta_{ik} - B_{ij} cos\Theta_{ik} \right] \quad i = j \quad (29)$$

$$\frac{\partial \Delta P_i}{\partial \Theta_j} = V_i V_j \left[ G_{ij} sin\Theta_{ij} - B_{ij} cos\Theta_{ij} \right] \quad i \neq j \quad (30)$$

$$\frac{\partial \Delta Q_i}{\partial \Theta_j} = V_i \sum_{k=1}^{n} |V_k| \left[ G_{ik} cos\Theta_{ik} + B_{ik} sin\Theta_{ik} \right] \quad i = j \quad (31)$$

$$\frac{\partial \Delta Q_i}{\partial \theta_j} = -V_i V_j [G_{ij} cos\theta_{ij} + B_{ij} sin\theta_{ij}] \quad i \neq j \tag{32}$$

Elements of $\Sigma_{reduced}$ matrix are given as below.

$$\frac{\partial P_{ij}}{\partial \theta_i} = -V_i V_j [G_{ij} sin\theta_{ij} + B_{ij} cos\theta_{ij}] \tag{33}$$

$$\frac{\partial P_{ij}}{\partial \theta_i} = V_i V_j [G_{ij} sin\theta_{ij} + B_{ij} cos\theta_{ij}] \tag{34}$$

$[\Sigma][\Phi] + [\Gamma]$ is a full rank matrix that indicates the relation between impedances and power flows. Most of the elements of this matrix are small and ineffective numbers. To be able to use sensitivity matrix as system control matrix, those ineffective numbers must be eliminated. This elimination process is defined at the next section.

## 3.2 System Control Matrix

System control matrix shows the relationship between inputs (line impedances) and outputs (real power flows) in a linearized manner. Since this matrix is used to determine minimum and maximum line impedances (inputs), and DSSC locations, this control matrix must be as accurate as possible. $[\Sigma][\Phi] + [\Gamma]$ is a full rank matrix that indicates the full relation between impedances and power flows, but most of the elements of this matrix are small and ineffective numbers. To be able to use power flow to impedance sensitivity matrix as system control matrix, those ineffective numbers must be eliminated. $[K]$ in (35) shows the system control matrix. (36) defines the control matrix as simplified power flow to impedance sensitivity matrix.

$$[\Delta P] = [K][\Delta x] \tag{35}$$

$$[K] = ([\Sigma][\Phi] + [\Gamma])_{simplified} \tag{36}$$

The negligible elements of sensitivity matrix are eliminated in two steps. First, the elements of each the row that is smaller than 25% of the maximum value are eliminated to determine the effective impedances on each line's power flow. Then the elements of the matrix that are smaller than 0.33 are eliminated, to determine the uncontrollable lines. As a result, sensitivity matrix is simplified and used as system control matrix.

Columns whose elements are all zero show the ineffective impedances. Other effective impedances will be controlled by placing DSSC devices. Rows whose elements are all zero show the uncontrollable lines. It must be noted that DSSC devices provides distributed support, and can be placed on a certain line more efficiently to improve the voltage stability. In this study, only consideration is real power flow control, so that DSSC devices are placed on lines uniformly.

## 3.3 Coupling Index

Since power system is an interconnected system, most of the line flows are related to each other. To be able to control power flows of the lines, correlation among the lines must be known. Coupling index can be used to determine the relationship among lines. Coupling can be determined by comparing the cosine of angles of vectors [17]. The cosine of the angle between two row vectors $v_1$ and $v_2$ of the total power flow to impedance sensitivity matrix is called coupling index [11].

$$cos\theta_{v_1.v_2} = \frac{v_1.v_2}{\|v_1\|\|v_2\|} \tag{37}$$

Coupling index can be used to determine the independently controllable lines [11]. Coupling index can also be used to calculate the final flows of the uncontrolled lines to determine whether they overload due to a certain control. Because it is really important to ensure that none of the lines will be overloaded after the control is applied. Otherwise, this control may lead to a brownout or even a blackout. In this

study, he coupling index is used to determine the final flows of uncontrolled lines. Equation (38) is used when only one line is controlled.

$$P_n{}^{last} = P_n{}^{initial} + [CI]_{(a,n)}P_n{}^{initial} \qquad n = 1 \dots L \qquad (38)$$

In (38), $P_n{}^{last}$ is final power flow of line n. $P_n{}^{initial}$ is the flow of the line before the control is applied. *CI* is the system coupling index matrix. L is the number of lines. (39) can be used when more than one line is controlled. In (39), m indicates the number of lines that is controlled.

$$P_n{}^{last} = P_n{}^{initial} + \left([CI]_{(a_1,n)} + [CI]_{(a_2,n)} + \dots + [CI]_{(a_m,n)}\right)P_n{}^{initial} \qquad n =$$
$$1 \dots L \quad (39)$$

Since the coupling index is calculated using linearized equations, although it shows realistic results for small impedance change, it does not show credible results when the power flow control exceeds 5%. Therefore, the power flow control is limited to 5% in this study. When it is necessary to apply a control over 5%, more controls must be applied consecutively. This may not be a problem if the algorithm is fast enough in real time.

Figure 10 shows a 5 bus test system, data of which are given at Tables 2 and 3. This sample 5 bus system is used to show the accuracy of the coupling index. First the coupling index matrix of the system is calculated under given operating conditions. Then the reactance of each line is increased separately, and the percentage changes of couplings among the lines are calculated. Results are presented at Table 4. As it can be seen from the Table 4, reactances of lines 2, 5 and 6 affect the couplings among the lines, whereas, reactances of lines 1, 3 and 4 do not have an important effect on couplings.
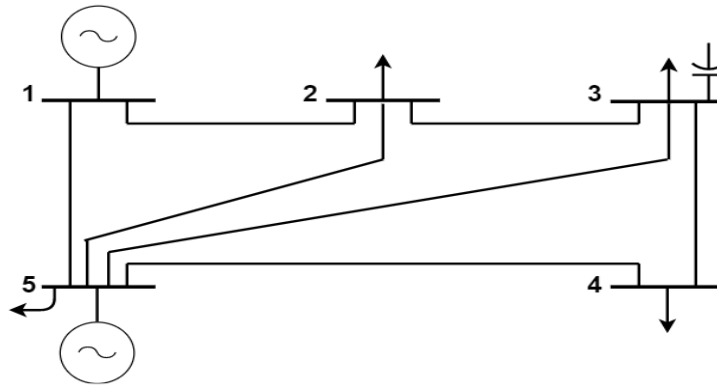
*Figure 10 5 Bus Test System*

*Table 2 5 Bus Test System Line Data*

| Line number | From bus | To bus | Resistance (Ohm) | Reactance (Ohm) | Susceptance (Siemens) |
|---|---|---|---|---|---|
| 1 | 1 | 2 | 0.02 | 0.10 | 0 |
| 2 | 1 | 5 | 0.05 | 0.25 | 0 |
| 3 | 2 | 3 | 0.04 | 0.20 | 0 |
| 4 | 2 | 5 | 0.05 | 0.25 | 0 |
| 5 | 3 | 4 | 0.05 | 0.25 | 0 |
| 6 | 3 | 5 | 0.08 | 0.40 | 0 |
| 7 | 4 | 5 | 0.10 | 0.50 | 0 |

*Table 3 5 Bus System Bus Data*

| Bus no. | Bus voltage | | Power generated | | Load | |
|---|---|---|---|---|---|---|
| | Magnitude (pu) | Angle (deg) | P (MW) | Q (MVAr) | P (MW) | P (MVAr) |
| 1 | 1.05 | 0 | 127 | 97 | 0 | 0 |
| 2 | 0.96 | -5 | 0 | 0 | 96 | 62 |
| 3 | 0.96 | -7 | 0 | 20 | 35 | 14 |
| 4 | 0.95 | -6 | 0 | 0 | 16 | 8 |
| 5 | 0.99 | -1.7 | 48 | 0 | 24 | 11 |

*Table 4 5 Bus Test System Change of Line Correlations Due to Impedance Change*

| Lines | Initial Correlations | | | | | |
|---|---|---|---|---|---|---|
| | 1 | 2 | 3 | 4 | 5 | 6 |
| 1 | 1.0 | -1.0 | -1.0 | -0.9 | 1.0 | 0.9 |
| 2 | -1.0 | 1.0 | 1.0 | 0.9 | -1.0 | -0.9 |
| 3 | -1.0 | 1.0 | 1.0 | 0.9 | -1.0 | -0.9 |
| 4 | -0.9 | 0.9 | 0.9 | 1.0 | -0.8 | -1.0 |
| 5 | 1.0 | -1.0 | -1.0 | -0.8 | 1.0 | 0.8 |
| 6 | 0.9 | -0.9 | -0.9 | -1.0 | 0.8 | 1.0 |
| | Percent correlation changes after imp. of line 1 is changed | | | | | |
| 1 | 0.0 | 0.0 | 0.0 | 1.3 | 0.4 | 1.2 |
| 2 | 0.0 | 0.0 | 0.0 | 1.4 | 0.4 | 1.3 |
| 3 | 0.0 | 0.0 | 0.0 | 1.3 | 0.4 | 1.2 |
| 4 | 1.3 | 1.4 | 1.3 | 0.0 | 3.8 | 0.0 |
| 5 | 0.4 | 0.4 | 0.4 | 3.8 | 0.0 | 3.6 |
| 6 | 1.2 | 1.3 | 1.2 | 0.0 | 3.6 | 0.0 |
| | Percent correlation changes after imp. of line 2 is changed | | | | | |
| 1 | 0.0 | 0.0 | 0.0 | 7.9 | 2.1 | 7.6 |
| 2 | 0.0 | 0.0 | 0.0 | 8.1 | 2.1 | 7.9 |
| 3 | 0.0 | 0.0 | 0.0 | 8.0 | 2.1 | 7.7 |
| 4 | 7.9 | 8.1 | 8 | 0 | 21.4 | 0 |
| 5 | 2.1 | 2.1 | 2.1 | 21.4 | 0 | 20.9 |
| 6 | 7.6 | 7.9 | 7.7 | 0 | 20.9 | 0 |
| | Percent correlation changes after imp. of line 3 is changed | | | | | |
| 1 | 0 | 0 | 0 | 5.6 | 1.6 | 5.5 |
| 2 | 0 | 0 | 0 | 5.8 | 1.5 | 5.6 |
| 3 | 0 | 0 | 0 | 5.7 | 1.5 | 5.5 |
| 4 | 5.6 | 5.8 | 5.7 | 0 | 15.2 | 0 |
| 5 | 1.6 | 1.5 | 1.5 | 15.2 | 0 | 14.9 |

| Lines | 1 | 2 | 3 | 4 | 5 | 6 |
|---|---|---|---|---|---|---|
| 6 | 5.5 | 5.6 | 5.5 | 0 | 14.9 | 0 |
| | Percent correlation changes after imp. of line 4 is changed | | | | | |
| 1 | 0 | 0 | 0 | 1.1 | -2.2 | 1 |
| 2 | 0 | 0 | 0 | 1.2 | -2.2 | 1.1 |
| 3 | 0 | 0 | 0 | 1.1 | -2.2 | 1.1 |
| 4 | 1.1 | 1.2 | 1.1 | 0 | -4.8 | 0 |
| 5 | -2.2 | -2.2 | -2.2 | -4.8 | 0 | -4.8 |
| 6 | 1 | 1.1 | 1.1 | 0 | -4.8 | 0 |
| | Percent correlation changes after imp. of line 5 is changed | | | | | |
| 1 | 0 | 0 | 0 | -91.3 | 0.5 | -90.1 |
| 2 | 0 | 0 | 0 | -91.3 | 0.4 | -90.1 |
| 3 | 0 | 0 | 0 | -90.9 | 0.4 | -89.8 |
| 4 | -91.3 | -91.3 | -90.9 | 0 | -120.5 | 0 |
| 5 | 0.5 | 0.4 | 0.4 | -120.5 | 0 | -119 |
| 6 | -90.1 | -90.1 | -89.8 | 0 | -119 | 0 |
| | Percent correlation changes after imp. of line 6 is changed | | | | | |
| 1 | 0 | 0 | 0 | 0.1 | -14.5 | 0.3 |
| 2 | 0 | 0 | 0 | -0.1 | -14.1 | 0.1 |
| 3 | 0 | 0 | 0 | -0.3 | -13.9 | -0.1 |
| 4 | 0.1 | -0.1 | -0.3 | 0 | -35 | 0 |
| 5 | -14.5 | -14.1 | -13.9 | -35 | 0 | -34.2 |
| 6 | 0.3 | 0.1 | -0.1 | 0 | -34.2 | 0 |

## 3.4 Transient Stability

It is well known that power flow control affects the transient stability. By applying the proper control, power oscillation damping and transient stability improvement can be achieved. On the other hand, any control may lead to catastrophic results in terms of stability. Therefore, before applying a certain control to the system, some points regarding the system stability must be considered. Transient response of the

system to a sudden impedance change depends on X/R ratio and the magnitude of the line current at that moment. If DSSC devices are introduced at the moment that line current is zero, zero transient should be achieved, because initial DC component is minimum when line current is zero [18]. X/R ratio of the lines and stability has a reverse relationship. Therefore, by reducing the impedance of lines, stability should be increased [19]. By considering the X/R ratio and line current's instant magnitude, controls can be achieved without any stability deterioration.

## 3.5 Conclusion

In order to achieve the desired control over the system, DSSC devices must be placed effectively. To do so, linear sensitivities can be used. But first, sensitivity matrix must be simplified to obtain a meaningful result. Once devices are placed, correlations among the lines must be known. Using this correlations, independently controllable lines and potential overloads can be determined.

# CHAPTER 4

## THE PROPOSED CONTROL ALGORITHM

The proposed algorithm calculates the effective DSSC locations using the system sensitivity matrix. Number of devices and minimum impedance intervals are calculated when the system is 90% loaded to ensure 10% control over real power flows of lines. Under normal conditions, when there is no overload, algorithm applies loss minimization to the whole system. This loss minimization provides additional benefit to cover the investment cost.

### 4.1 Power Flow Control

As the power systems are interconnected, and have meshed structures; any line's power flow does not depend only on its own impedance, such that it may depend on more than five impedances for a large system. Therefore, to be able to control a power flow, final values of the more than 5 impedances must be calculated. However, only the final impedance value of the line that will be controlled is known. Therefore, one cannot calculate the final values of all the impedances directly, but rather should solve an optimization problem. Optimization problem for power flow control is as follows.

$$f(x) = \sum_{n=1}^{L} \left( P_{n,calculated} - P_{n,desired} \right)^2$$

$$\min f$$

$$St \quad f_{(p,q)}\left( s_{(\Theta,v)} \right) = 0 \tag{40}$$

$$x \leq x_{max}$$
$$x \geq x_{min}$$

In (40), $P_{flow,ij}$ is power flow between line i and j, $x_{min}$ and $x_{max}$ are minimum and maximum line impedances. $f_{(p,q)}$ is real and reactive power balance equations. Objective function, f(.) is the square of difference between the desired and calculated real power flows. Constraints are real power balance equations and minimum and maximum line impedances. As it can be seen from the equation (40), the reactive power balance equations are neglected, because reactive power balance of the system is barely changed thanks to the series compensation prided by DSSCs, which is negligible. Neglecting reactive power balance equations makes a great contribution to the total calculation time of power flow control, since the gradient is calculated at each iteration; total calculation time reduces significantly, as much as 30%.

## 4.2 Loss Minimization

All of the DSSC devices will not be used for power flow control all the time; therefore, loss minimization can be achieved by using the unused devices to compensate the investment cost. Optimization problem that is used for loss minimization is as follows:

$$P_{loss} = \sum_{i}^{n} \sum_{j}^{n} P_{flow,ij} \qquad i \neq j$$
$$\min P_{loss}$$
$$St \quad f_{(p,q)}\big(s_{(\Theta,v)}\big) = 0 \tag{41}$$
$$x \leq x_{max}$$
$$x \geq x_{min}$$

Constraints of loss minimization are real and reactive power balance equations, impedance limits and real power flow limits.

Both power flow control and loss minimization problems can be solved using gradient search method using the sensitivities as gradients. The gradient search optimization approach is a logical choice because it requires only knowledge of the sensitivities and the ability to solve the power flow, and it guarantees movement toward the optimum [11]. Steps of gradient search can be defined as follows.

$$x^{i+1} = x^i + \alpha \nabla f(x^i) \qquad \alpha > 0 \tag{42}$$

x is impedances, $\alpha$ is step size and $\nabla f$ is the gradient of the objective function. Step size of each gradient must be determined to optimize the algorithm. Gradient of power flow control is defined below.

$$\nabla f(x) = \frac{\partial P_{ij}}{\partial x_l}^{full} = \frac{\partial P_{ij}}{\partial S(\Theta,V)}\frac{\partial S(\Theta,V)}{\partial x_l} + \frac{\partial P_{ij}}{\partial x_l} \tag{43}$$

This equation is ij$^{th}$ row of the power flow to impedance sensitivity matrix. This equation can be simplified to reduce the calculation time. It will be seen later that although bus voltage magnitudes are sensitive to impedance change, impedance change has very small effect on voltage magnitudes; therefore, voltage magnitudes can be eliminated from this equation. New gradient becomes as follows:

$$\nabla f(x) = \frac{\partial P_{ij}}{\partial x_l}^{full} = \frac{\partial P_{ij}}{\partial S(\Theta)}\frac{\partial S(\Theta)}{\partial x_l} + \frac{\partial P_{ij}}{\partial x_l} \tag{44}$$

This reduction made a great contribution to the calculation time of power flow control since the gradient is calculated at every iteration.

Gradient of loss minimization:

$$\nabla f(x) = \frac{\partial P_{loss}}{\partial x_l} = \sum_{i=1}^{N} \sum_{j=1}^{N} \frac{\partial P_{ij}}{\partial S(\Theta,V)} \frac{\partial S(\Theta,V)}{\partial x_l} + \frac{\partial P_{ij}}{\partial x_l} \quad i \neq j \tag{45}$$

This gradient can be calculated using the system sensitivity matrix. To calculate this, sensitivity matrix must be calculated twice. Since the gradient is calculated every iteration, sensitivity matrix is a complex matrix and loss minimization is applied to whole system, loss minimization takes a long time. Instead of using sensitivity as gradient, new gradient can be defined to reduce the duration of loss minimization.

$$\nabla f(x) = \sum \left( \frac{\partial P_{ij}}{\partial S(\Theta,V)} + \frac{\partial P_{ji}}{\partial S(\Theta,V)} \right) \frac{\partial S(\Theta,V)}{\partial x_l} + \frac{\partial P_{ij}}{\partial x_l} + \frac{\partial P_{ji}}{\partial x_l} \quad i \neq j \tag{46}$$

Using this gradient instead of sensitivities shortened the calculation time about 80%.

## 4.3 Proposed Algorithm

- Controllability margin is defined as 10% of the line impedance.
- System controllability matrix is calculated by simplifying the sensitivity matrix when the system is 90% loaded. By using controllability matrix, DFACTS locations and uncontrollable lines are determined. Then, by using controllability matrix, minimum and maximum line impedances are calculated to determine the necessary number of devices per line. Equation (42) is used to calculate the number of devices.

$$Number\ of\ devices\ per\ phase = \frac{S_B \Delta X^{pu} (I_{line}{}^{pu})^2}{3 Q_{DSSC}} \tag{42}$$

Once DSSC number is calculated, minimum and maximum line impedances must be updated if line current changes, because injected impedance by DSSC depends on the line current. The line impedance limits are calculated using equations (43) and (44).

$$x_{min}{}^n = x_0{}^n - \frac{3(number\ of\ devices)Q_{DSSC}}{S_B(I_{line}{}^{pu})} \quad n = 1 \ldots L \tag{43}$$

$$x_{max}{}^n = x_0{}^n + \frac{3(number\ of\ devices)Q_{DSSC}}{S_B(I_{line}{}^{pu})} \quad n = 1 \ldots L \tag{44}$$

In equations (42), (43) and (44), $S_B$, $I_{line}{}^{pu}$, $Q_{DSSC}$ and $x_0{}^n$ are base power, line current in pu, reactive power of DSSC in kVA, reactance of n. line in pu, respectively.

- Algorithm always checks for overload. If there is not any overload, loss minimization algorithm works continuously.

- Loss minimization algorithm: Variables of the loss minimization algorithm are lines with DSSCs that is not being used for power flow control. During the loss minimization if an overload occurs, program goes to power flow control, equalizes the overloaded lines power flow to the maximum value. If loss between two consecutive loops changes less than 0.0003 MW, loss minimization algorithm stops.

- Power flow control algorithm: During the loss minimization or normal operation if one or more lines overloads, power flow algorithm starts. First line controllability is checked. If overloaded line or lines are controllable, and if there are at least two lines to be controlled, program checks the coupling index to determine the whether those lines are independently controllable. We assumed that if the coupling index is less than 0.1, lines are independently controllable. Then, by using coupling index, whether any line can overload due to this control is determined. If the control is feasible, power flow control can be applied. Because of coupling index is not so accurate, some of the lines should overload during the power flow control in 0.1-0.2% level. This overload can be fixed after the power flow finishes. It's not possible to intervene to other lines during the algorithm as in loss minimization.

- Control algorithm is used to check whether lines can actually be controlled 10%. It's assumed that if difference between the final power flow and desired power flow is less than 1% of desired power flow, that line is controllable.

Figure 11 presents the flowchart of proposed algorithm.
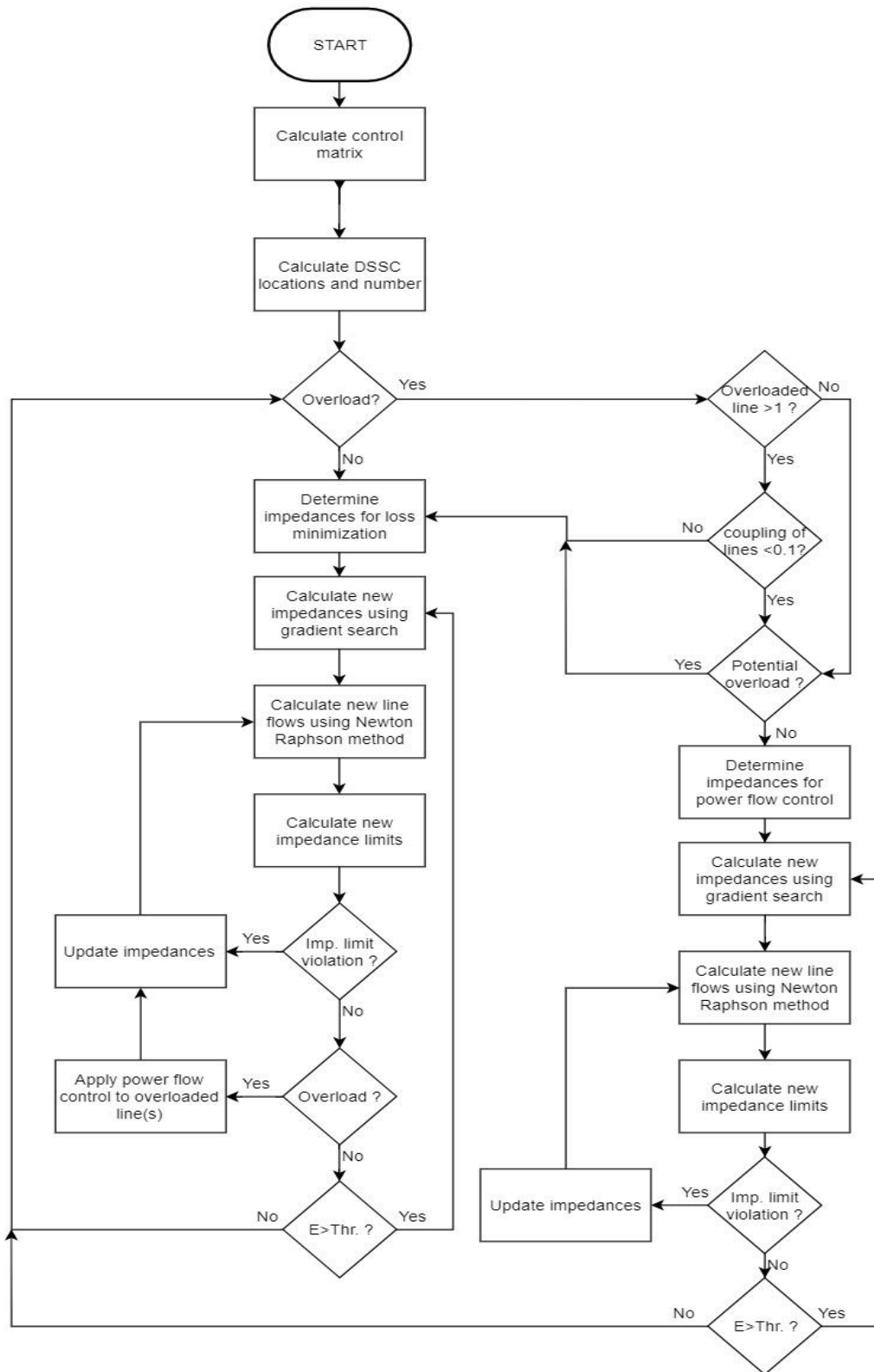
*Figure 11 Flowchart of Proposed Algorithm*

# CHAPTER 5

# SIMULATION

Proposed algorithm is tested at IEEE 14 bus and IEEE 30 bus test systems with three cases. Those cases are 90% loading, 70% loading and 50% loading conditions.

## 5.1 IEEE 14 Bus Test System

Figure 12 shows the schematic diagram of IEEE 14 bus test system. System's line data is presented at Table 5.



*Figure 12 IEEE 14 Bus Test System*

### 5.1.1    14 Bus 90% Load Conditions with Constant Impedance Intervals

IEEE 14 bus system's bus voltage magnitudes and phase angles, load and generation information under 90% load are presented at Table 6.

*Table 5 IEEE 14 Bus Test System Line Data*

| Line number | From bus | To bus | Resistance (pu) | Reactance (pu) | Susceptance (pu) |
|---|---|---|---|---|---|
| 1 | 1 | 2 | 0.0194 | 0.0592 | 0.0528 |
| 2 | 1 | 5 | 0.0540 | 0.2230 | 0.0492 |
| 3 | 2 | 5 | 0.0570 | 0.1739 | 0.0340 |
| 4 | 2 | 4 | 0.0581 | 0.1763 | 0.0374 |
| 5 | 2 | 3 | 0.0470 | 0.1980 | 0.0438 |
| 6 | 4 | 3 | 0.0670 | 0.1710 | 0.0346 |
| 7 | 5 | 6 | 0.0000 | 0.2520 | 0.0000 |
| 8 | 5 | 4 | 0.0134 | 0.0421 | 0.0128 |
| 9 | 4 | 9 | 0.0000 | 0.5562 | 0.0000 |
| 10 | 4 | 7 | 0.0000 | 0.2091 | 0.0000 |
| 11 | 7 | 8 | 0.0000 | 0.1762 | 0.0000 |
| 12 | 7 | 9 | 0.0000 | 0.1100 | 0.0000 |
| 13 | 9 | 10 | 0.0318 | 0.0845 | 0.0000 |
| 14 | 9 | 14 | 0.1271 | 0.2704 | 0.0000 |
| 15 | 11 | 10 | 0.0821 | 0.1921 | 0.0000 |
| 16 | 6 | 11 | 0.0950 | 0.1989 | 0.0000 |
| 17 | 6 | 12 | 0.1229 | 0.2558 | 0.0000 |
| 18 | 6 | 13 | 0.0662 | 0.1303 | 0.0000 |
| 19 | 12 | 13 | 0.2209 | 0.1999 | 0.0000 |
| 20 | 13 | 14 | 0.1709 | 0.3480 | 0.0000 |

*Table 6 IEEE 14 Bus Test System Bus Data under 90% Load*

| Bus number | Bus voltage | | Load | | Generation | |
|---|---|---|---|---|---|---|
| | Magnitude (pu) | Phase angle (degree) | Real power (MW) | Reactive power (MVAR) | Real power (MW) | Reactive power (MVAR) |
| 1 | 1.06 | 0 | 0 | 0 | 232.28 | -16.89 |
| 2 | 1.045 | -4.98 | 21.7 | 12.7 | 40 | 42.39 |
| 3 | 1.01 | -12.72 | 94.2 | 19 | 0 | 23.39 |
| 4 | 1.0186 | -10.32 | 47.8 | -3.9 | 0 | 0 |
| 5 | 1.0203 | -8.78 | 7.6 | 1.6 | 0 | 0 |
| 6 | 1.07 | -14.22 | 11.2 | 7.5 | 0 | 12.22 |
| 7 | 1.062 | -13.37 | 0 | 0 | 0 | 0 |
| 8 | 1.09 | -13.37 | 0 | 0 | 0 | 17.36 |
| 9 | 1.0563 | -14.95 | 29.5 | 16.6 | 0 | 0 |
| 10 | 1.0513 | -15.1 | 9 | 5.8 | 0 | 0 |
| 11 | 1.0571 | -14.79 | 3.5 | 1.8 | 0 | 0 |
| 12 | 1.0552 | -15.08 | 6.1 | 1.6 | 0 | 0 |
| 13 | 1.0505 | -15.16 | 13.5 | 5.8 | 0 | 0 |
| 14 | 1.0358 | -16.04 | 14.9 | 5 | 0 | 0 |

Impedance intervals, line limits and DSSC locations are presented in Table 7. Minimum and maximum impedance intervals, number of devices and controllable lines are determined when the system is 90% loaded. As it is mentioned earlier, injected impedance directly depends on the line current. But to compare the results and calculation time, first we assumed impedance intervals are constant. After the impedance intervals are determined, loss minimization and then power flow control to lines 3 and 6 is applied. Final impedances, real power flows, loss minimization, voltage magnitude change and impedance changes are presented in the figures below. As it can be seen from Table 7, 1644 DSSC devices suffice to control lines by 10%. And only line between busses 7 and 8 is uncontrollable. 5 of the all lines

are not effective on power flow, therefore DSSC devices are not placed on those lines.

*Table 7 IEEE 14 Bus Test System Results*

| from | to | Xmin (pu) | Xmax (pu) | Plimit (MW) | Number of DSSC | Controllable |
|------|----|-----------|-----------|-------------|----------------|--------------|
| 1 | 2 | 0.0246 | 0.0937 | 172.3 | 940 | Yes |
| 1 | 5 | 0.2029 | 0.2432 | 83.4 | 129 | Yes |
| 2 | 5 | 0.1664 | 0.1814 | 45.6 | 15 | Yes |
| 2 | 4 | 0.1633 | 0.1894 | 61.7 | 46 | Yes |
| 2 | 3 | 0.1644 | 0.2316 | 80.5 | 200 | Yes |
| 4 | 3 | 0.1584 | 0.1836 | 26.1 | 8 | Yes |
| 5 | 6 | 0.2265 | 0.2775 | 47.9 | 54 | Yes |
| 5 | 4 | 0.0059 | 0.0783 | 68.7 | 157 | Yes |
| 4 | 9 | 0.5408 | 0.5716 | 17.8 | 5 | Yes |
| 4 | 7 | 0.1888 | 0.2294 | 31.5 | 19 | Yes |
| 7 | 8 | 0.1762 | 0.1762 | 0 | 0 | No |
| 7 | 9 | 0.0881 | 0.1319 | 31.5 | 20 | Yes |
| 9 | 10 | 0.0845 | 0.0845 | 6.2 | 0 | Yes |
| 9 | 14 | 0.2633 | 0.2774 | 10.6 | 1 | Yes |
| 11 | 10 | 0.1921 | 0.1921 | 3.7 | 0 | Yes |
| 6 | 11 | 0.1965 | 0.2013 | 7.7 | 1 | Yes |
| 6 | 12 | 0.2431 | 0.2685 | 8.6 | 1 | Yes |
| 6 | 13 | 0.0980 | 0.1625 | 19.4 | 12 | Yes |
| 12 | 13 | 0.1999 | 0.1999 | 1.8 | 0 | Yes |
| 13 | 14 | 0.3480 | 0.3480 | 6.0 | 0 | Yes |

After the controllable lines and impedance intervals are determined, loss minimization is applied. In this case, loss is reduced by 2.14% (0.2867 MW). Figure

13 shows iterations of loss minimization algorithm. Within 18 iterations, loss minimization is completed.
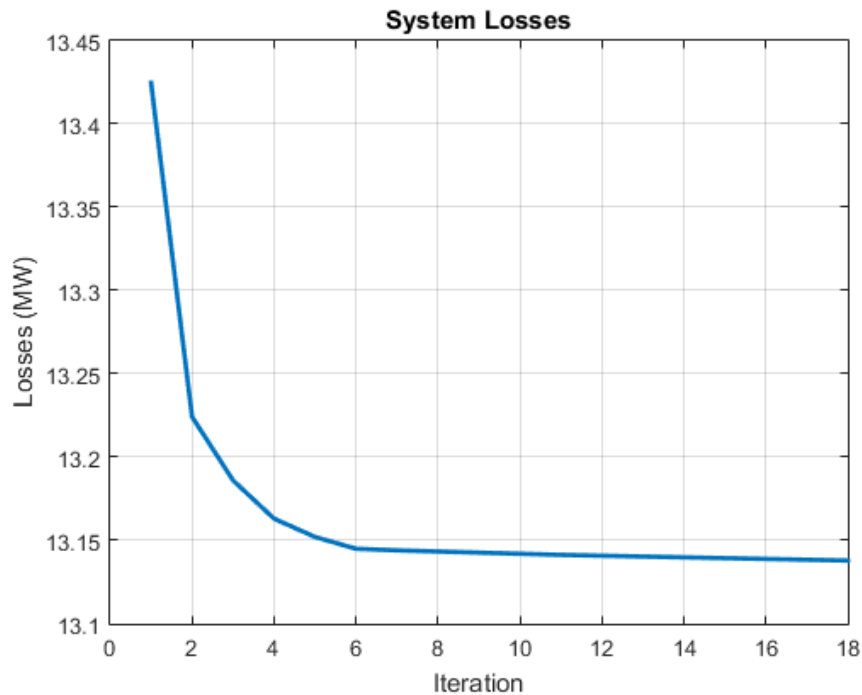


*Figure 13 IEEE 14 Bus System Under 90% Load with Constant Impedance Intervals Loss Minimization*

Then power flow control is applied to 1st and 7th lines to increase the power flows of those lines by 5%. Absolute value of the correlation between the lines is less than 0.1 (0.02), but algorithm detected that lines 5, 15, 16 and 20 might overload due to this control, and yet the control is applied to see whether those lines overload. Aforementioned lines are overloaded by 0.28, 28, 9.2 and 6.2 percent respectively. This result confirms our method to detect potential overloads before the control is applied. Then power flow control is applied to lines 3 and 6. Table 8 shows the results of power flow control. Desired power flows are achieved accurately.

*Table 8 IEEE 14 Bus System Power Flow Control*

| Controlled lines | Initial P | Desired P | Final P |
|---|---|---|---|
| 3 | 34.7183 | 38.19 | 38.19 |
| 6 | 17.24 | 18.97 | 18.91 |

As it can be seen from Table 8, power flow control over lines 3 and 6 is achieved simultaneously. More than two lines also can be controlled simultaneously if it's necessary, and the control is feasible. Figure 14 shows the line impedances after loss minimization and power flow control is applied. Red lines shows the minimum and maximum impedance limits and green line shows the final impedances. As it can be seen from the figure below, desired controls are achieved without any impedance violations.
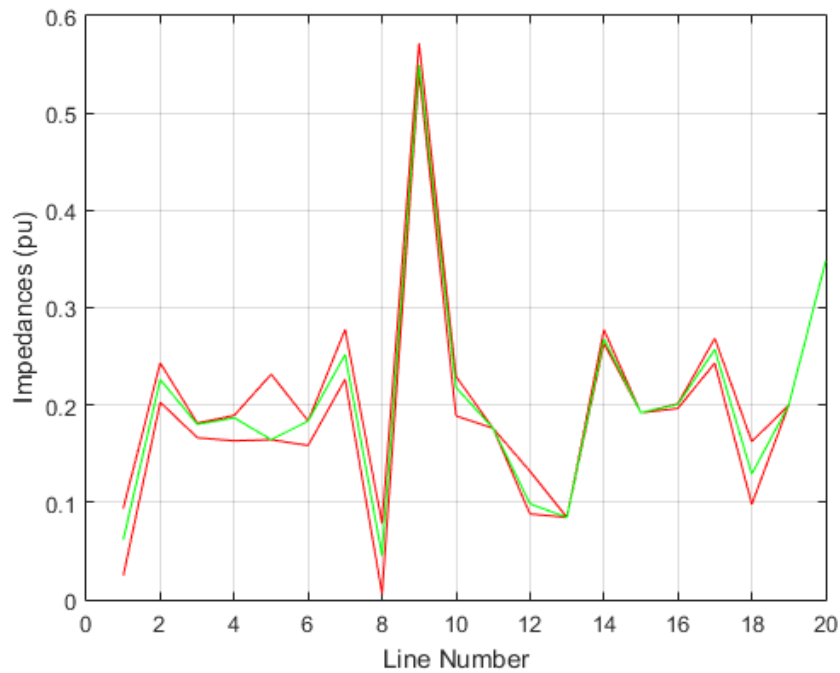


*Figure 14 IEEE 14 Bus System Under 90% Load With Constant Impedance Intervals Line Impedances After Loss Minimization and Power Flow Control*

Figures 15 and 16 show the voltage magnitude change and total impedance change after loss minimization and power flow control, respectively. After controls are applied, voltage magnitudes are changed less than 0.14% and line impedance changed less than 18%. Considering this, as it is mentioned earlier, voltage magnitudes are eliminated from gradient of power flow control algorithm. This elimination reduced the power flow control duration about 30%. Then the same thing is done for loss minimization algorithm, but loss minimization duration is increased. Therefore, voltage magnitudes are considered as a state while calculating gradient of loss minimization.
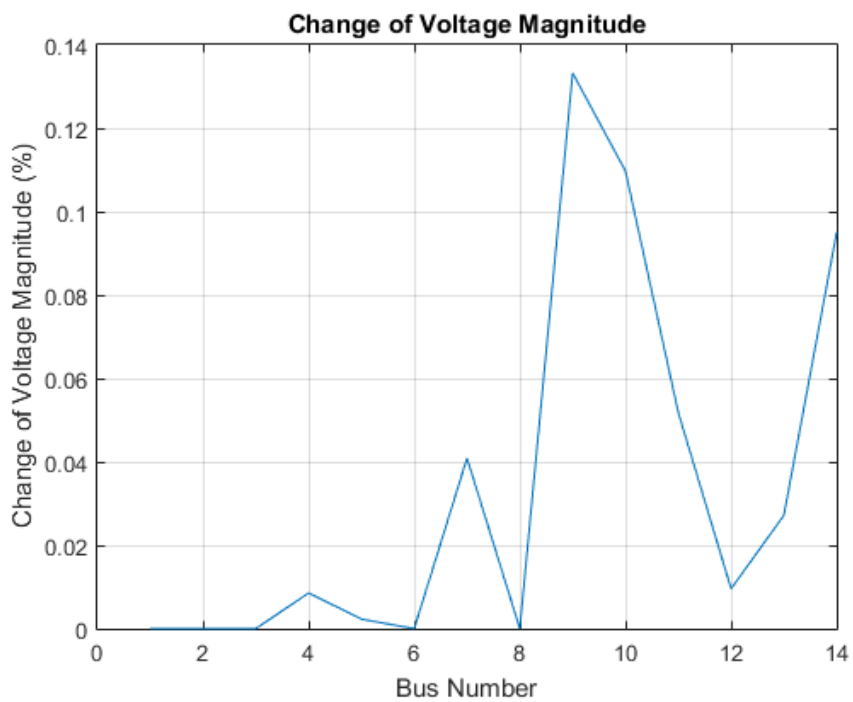


*Figure 15 IEEE 15 Bus System under 90% Load with Constant Impedance Intervals Voltage Magnitude Change due to Loss Minimization and Power Flow Control*
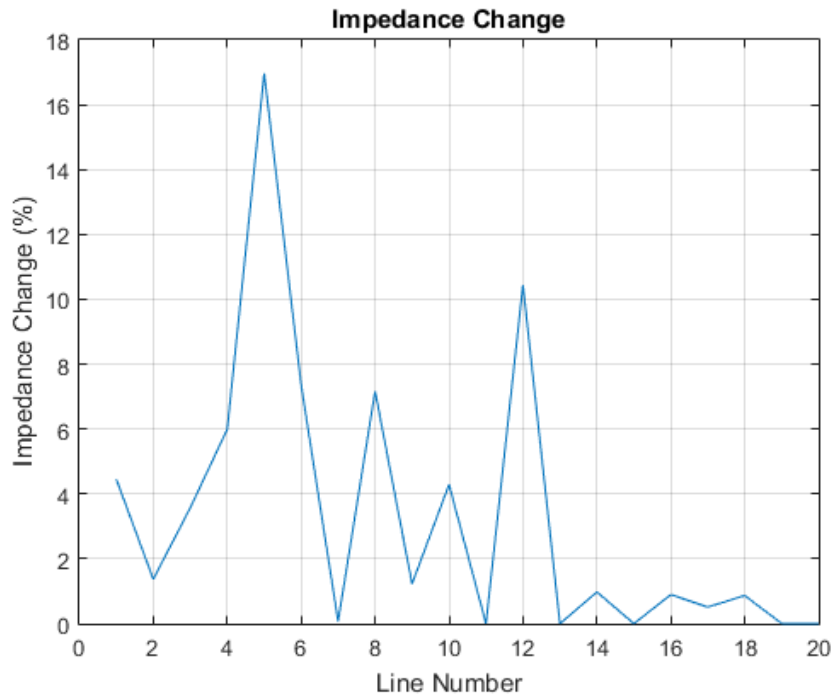
*Figure 16 IEEE 14 Bus System under 90% Load with Constant Impedance Intervals Impedance Change due to Loss Minimization and Power Flow Control*

### 5.1.2 14 Bus 90% Load Conditions with Variable Impedance Intervals

The same controls are applied with variable impedance intervals to compare the two situations in terms of calculation time and accuracy. First loss minimization is applied. Loss is reduced by 2.24% (0.3 MW). Figure 17 shows iterations of loss minimization algorithm. Calculation time of loss minimization is 1.24 seconds. Compared to constant impedance intervals case, loss is reduce 0.1% more. This clearly shows the advantage of variable impedance intervals, because as line currents reduce, impedance intervals increase, and this provides more control over the system.

44
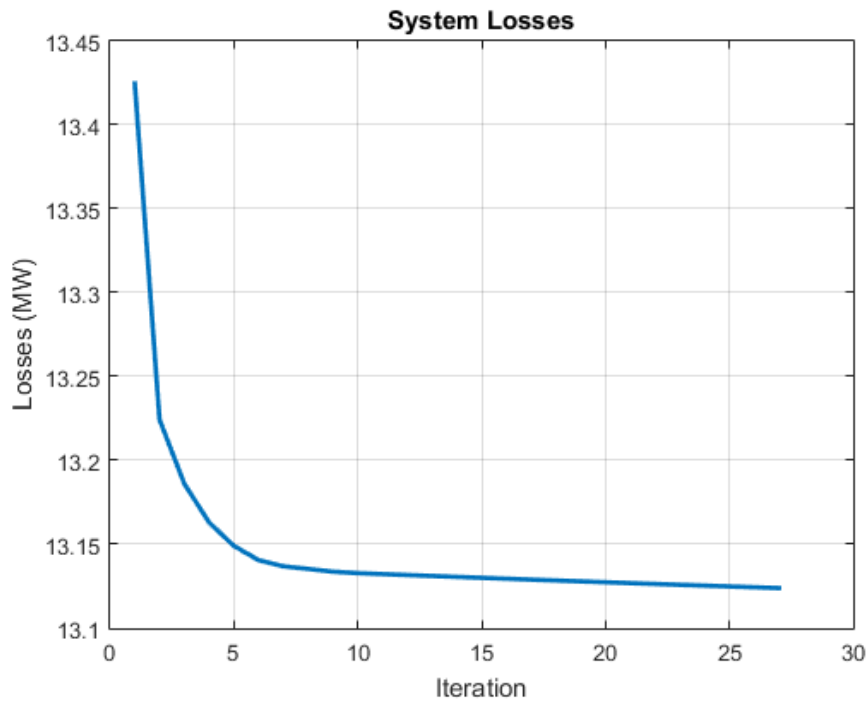
*Figure 17 IEEE 14 Bus System under 90% Load with Variable Impedance Intervals Loss Minimization*

Figures 18 and 19 show the line impedances and real power flows after loss minimization, respectively. In those figures, red lines shows the limits and green lines shows the actual values. As it can be seen from the figures below, loss minimization is achieved without any impedance and power flow limit violations despite the system is highly loaded.
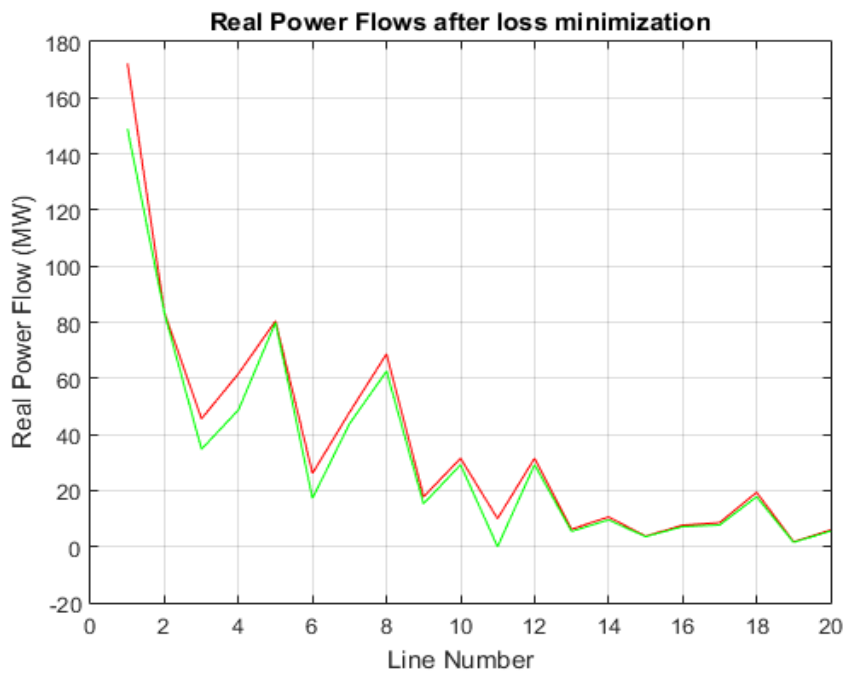
*Figure 18 IEEE 14 Bus System under 90% Load with Variable Impedance Intervals Real Power Flows after Loss Minimization*
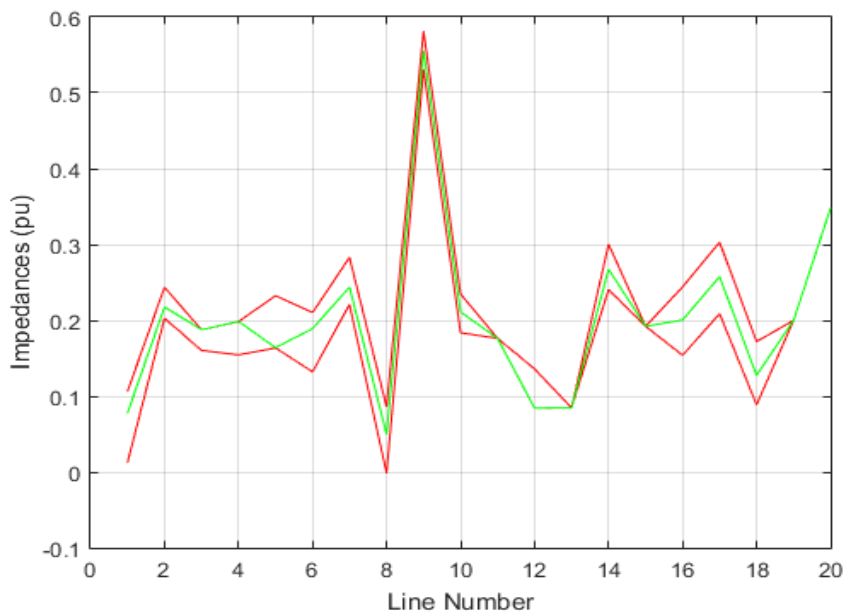


*Figure 19 IEEE 14 Bus System under 90% Load with Variable Impedance Intervals Line Impedances and Line Limits after Loss Minimization*

Then power flow control is applied to lines 3 and 6 which are independently controllable. Table 9 shows the results of power flow control.

*Table 9 IEEE 14 Bus System under 90% Load with Variable Impedance Intervals Power Flow Control*

| Controlled lines | Initial P | Desired P | Final P |
|---|---|---|---|
| 3 | 33.66 | 31.98 | 31.99 |
| 6 | 16.91 | 16.07 | 16.11 |

As it can be seen from Table 9, power flow control over lines 3 and 6 is achieved simultaneously. Power flows of those lines reduced by 5%. Figures 20 and 21 show the line impedances and real power flows after loss minimization and power flow control is applied, respectively. As it can be seen from the figures below, desired controls are achieved without any impedance and power flow limit violations.
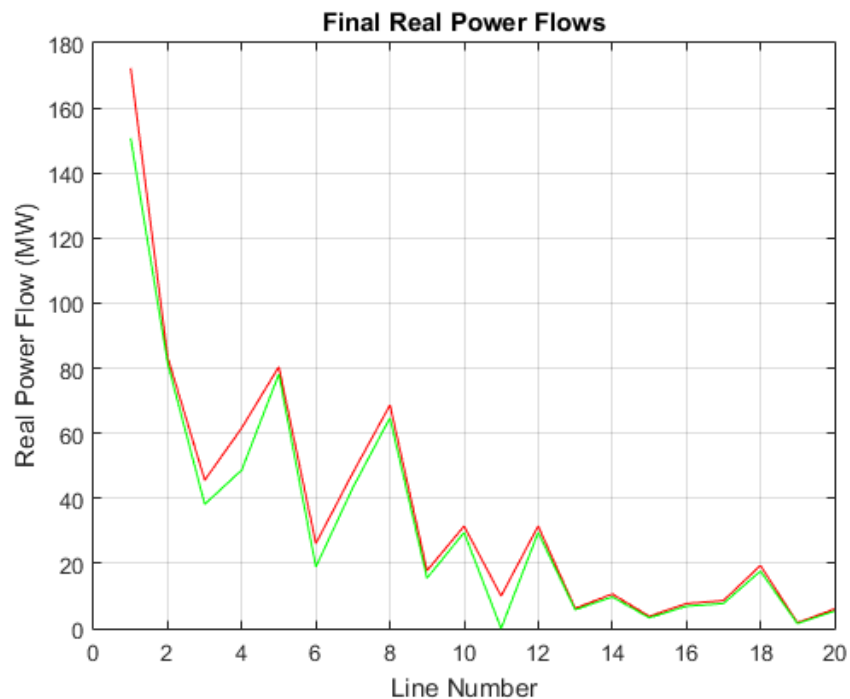


*Figure 20 IEEE 14 Bus System under 90% Load with Variable Impedance Intervals Final Real Power Flows after Loss Minimization and Power Flow Control*

47
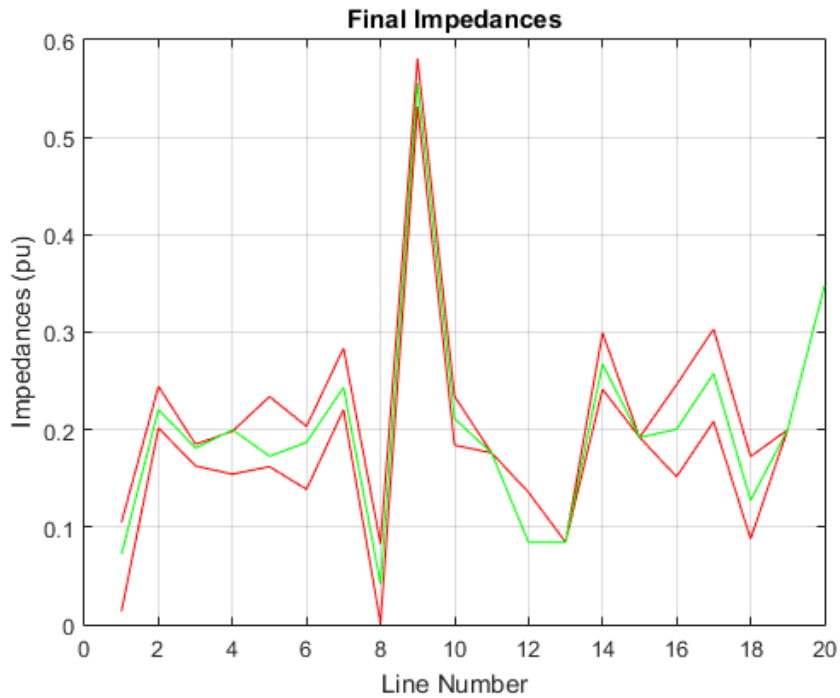
*Figure 21 IEEE 14 Bus System under 90% Load with Variable Impedance Intervals Real Line Impedances and Impedance Limits after Loss Minimization and Power Flow Control*

Figures 22 and 23 show the voltage magnitude change and total impedance change after loss minimization and power flow control, respectively. After controls are applied, voltage magnitudes are changed less than 0.3% and line impedance changed less than 25%. Voltage magnitudes are changed more than constant impedance intervals case, but still this change is very small. And since series compensation is feasible up to 80%, 25% impedance change is an acceptable result.
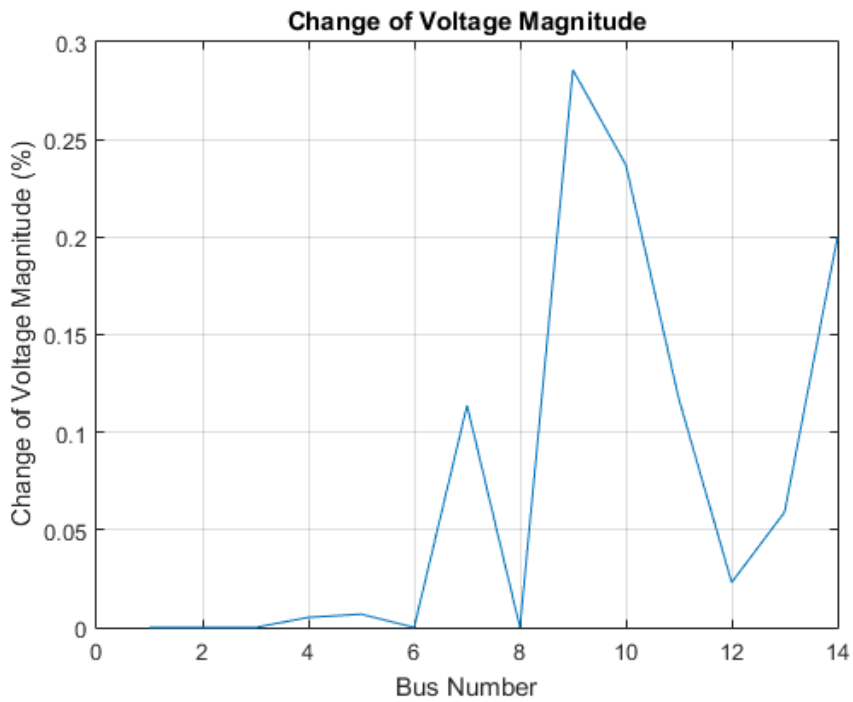
*Figure 22 IEEE 14 Bus System under 90% Load with Variable Impedance Intervals Change of Voltage Magnitude after Loss Minimization and Power Flow Control*
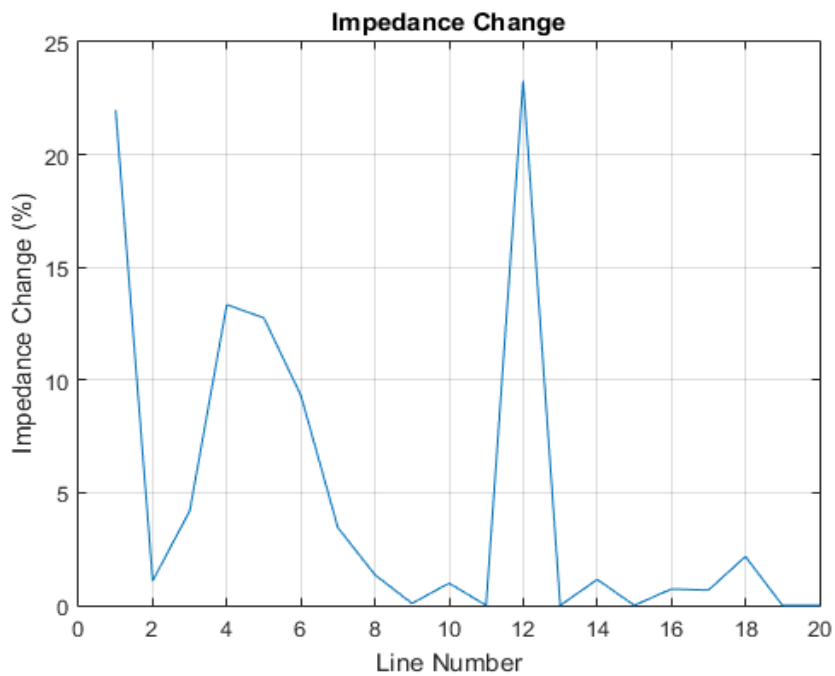


*Figure 23 IEEE 14 Bus System under 90% Load with Variable Impedance Intervals Change of Line Impedances after Loss Minimization and Power Flow Control*

### 5.1.3   14 Bus 70% load conditions

IEEE 14 bus system's bus voltage magnitudes and phase angles, load and generation information under 70% load are presented at Table 10.

First loss minimization is applied. Loss is reduced by 2.5% (0.16 MW). Figure 24 shows iterations of loss minimization algorithm. Calculation time of loss minimization is 1.27 seconds. In this case loss minimization took 0.03 seconds more than 90% percent load case. Also %loss minimization is increased and MW loss minimization is decreased as system load decreases by 20%.

*Table 10 IEEE 14 Bus Test System under 70% Load*

| Bus number | Bus voltage | | Generation | | Load | |
|---|---|---|---|---|---|---|
| | Magnitude (pu) | Phase angle (degree) | Real power (MW) | Reactive power (MVAR) | Real power (MW) | Reactive power (MVAR) |
| 1 | 1.06 | 0.00 | 0.00 | 0.00 | 162.60 | -11.82 |
| 2 | 1.05 | -3.54 | 15.19 | 8.89 | 28.00 | 29.67 |
| 3 | 1.02 | -8.74 | 65.94 | 13.30 | 0.00 | 16.37 |
| 4 | 1.04 | -7.26 | 33.46 | -2.73 | 0.00 | 0.00 |
| 5 | 1.04 | -6.64 | 5.32 | 1.12 | 0.00 | 0.00 |
| 6 | 1.05 | -10.49 | 7.84 | 5.25 | 0.00 | 8.55 |
| 7 | 1.05 | -9.62 | 0.00 | 0.00 | 0.00 | 0.00 |
| 8 | 1.09 | -9.62 | 0.00 | 0.00 | 0.00 | 12.15 |
| 9 | 1.04 | -10.69 | 20.65 | 11.62 | 0.00 | 0.00 |
| 10 | 1.03 | -10.86 | 6.30 | 4.06 | 0.00 | 0.00 |
| 11 | 1.04 | -10.77 | 2.45 | 1.26 | 0.00 | 0.00 |
| 12 | 1.04 | -11.09 | 4.27 | 1.12 | 0.00 | 0.00 |
| 13 | 1.04 | -11.12 | 9.45 | 4.06 | 0.00 | 0.00 |
| 14 | 1.02 | -11.60 | 10.43 | 3.50 | 0.00 | 0.00 |
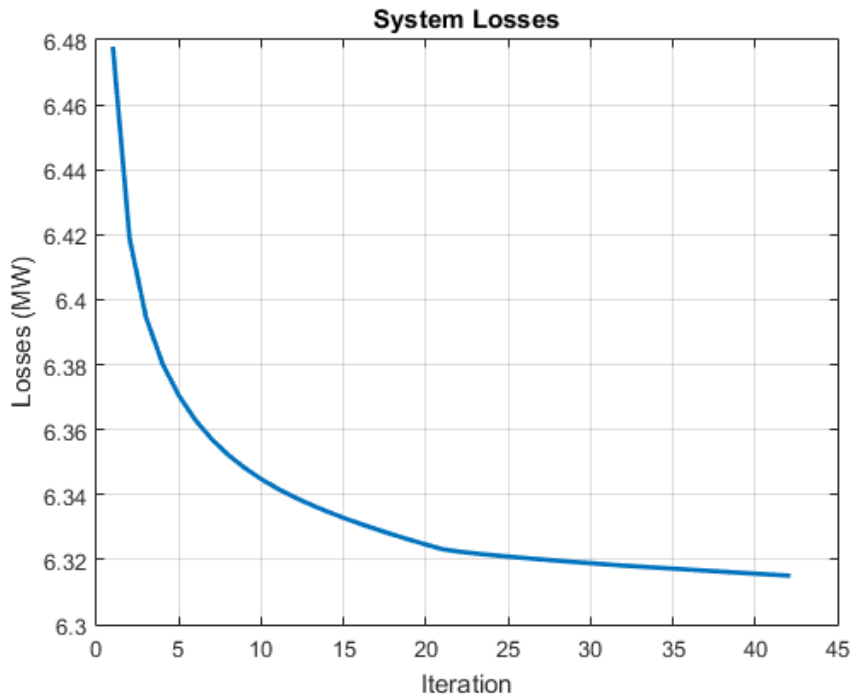
*Figure 24 IEEE 14 Bus System under 70% Load Loss Minimization*

Figures 25 and 26 show the line impedances and real power flows after loss minimization, respectively. As it can be seen from the figures below, loss minimization is achieved without any impedance and power flow limit violations. Comparing to the 90% load case, impedance intervals increased as line currents decreased.

*Figure 25 IEEE 14 Bus System under 70% Load Real Power Flows After Loss Minimization*
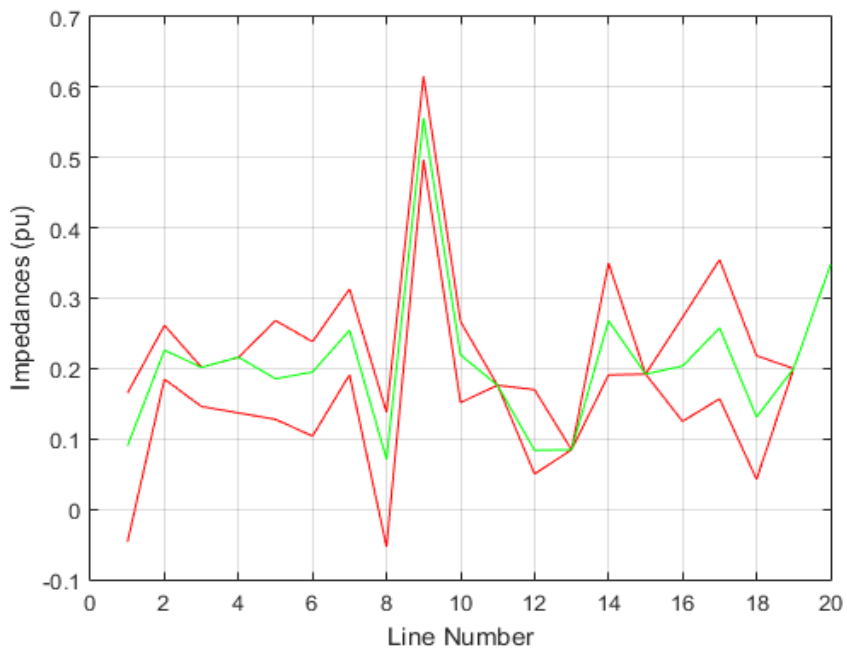


*Figure 26 IEEE 14 Bus System under 70% Load Line Impedances and Impedance Limits after Loss Minimization*

52

Then power flow control is applied to lines 3 and 6 which are independently controllable. Power flows of lines 3 and 6 increased by 50%. Since load is 70% and system is relived, 50% control over the lines could be achieved accurately. Table 11 shows the results of power flow control.

*Table 11 IEEE 14 Bus System under 70% Load Power Flow Control*

| Controlled lines | Initial P | Desired P | Final P |
|---|---|---|---|
| 3 | 21.9 | 30.67 | 30.67 |
| 6 | 12.99 | 18.18 | 18.12 |

As it can be seen from Table 11, power flow control over lines 3 and 6 is achieved simultaneously. Figures 27 and 28 show the real power flows and line impedances after loss minimization and power flow control is applied, respectively. As it can be seen from the figures below, desired controls are achieved without any impedance and power flow limit violations. It must be noted that, as system load reduced from 90% to 70%, power flow control margin is increased. In this case, 50% power flow control is applied to lines 3 and 6 while in 90% load case, applied control was only 5%. Because, when system is heavily loaded, any control may lead to congestion, therefore, applied controls must be less than 5%.
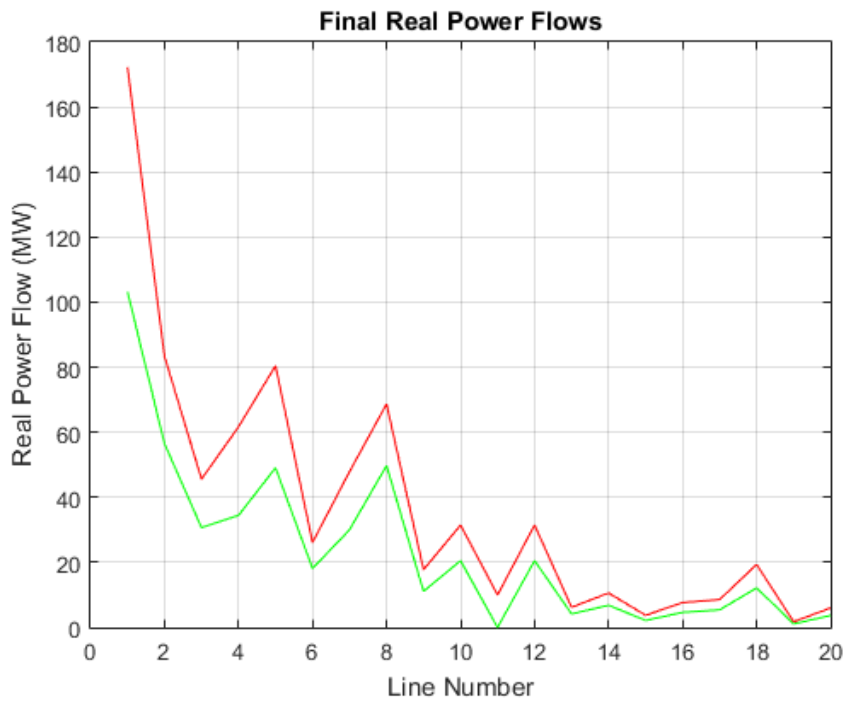
*Figure 27 IEEE 14 Bus System under 70% Load Final Real Power Flows after Loss Minimization and Power Flow Control*
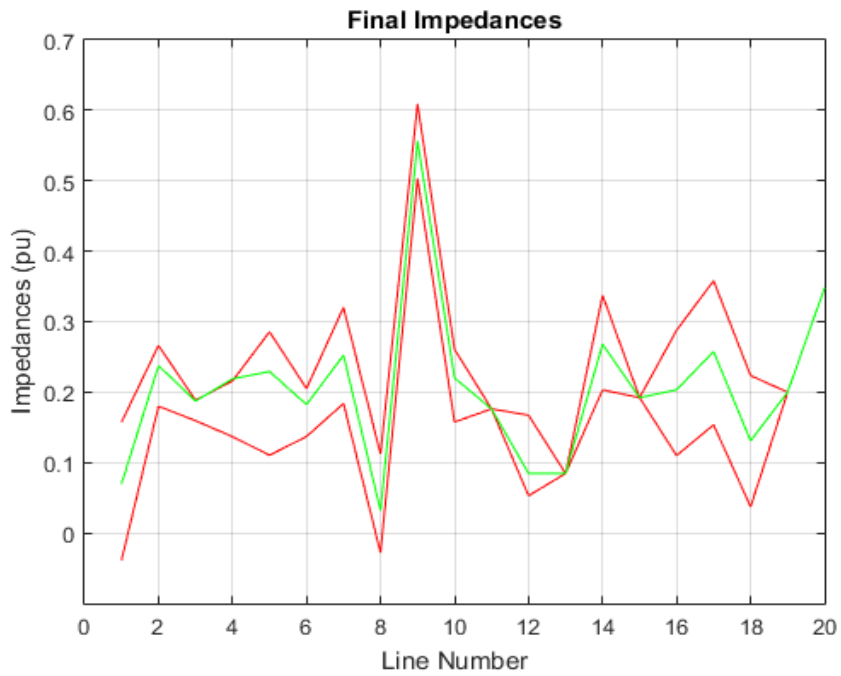


*Figure 28 IEEE 14 Bus System under 70% Load Final Line Impedances and Impedance Limits after Loss Minimization and Power Flow Control*

Figures 29 and 30 show the voltage magnitude change and total impedance change after loss minimization and power flow control, respectively. After controls are applied, voltage magnitudes are changed less than 0.25% and line impedance changed less than 25%.
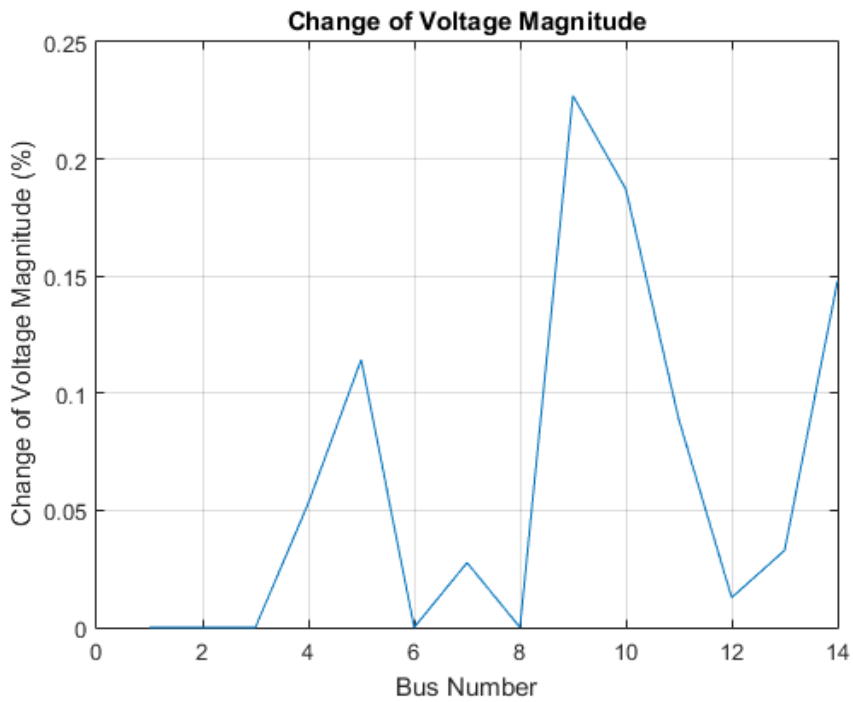


*Figure 29 IEEE 14 Bus System under 70% Load Change of Voltage Magnitudes after Loss Minimization and Power Flow Control*
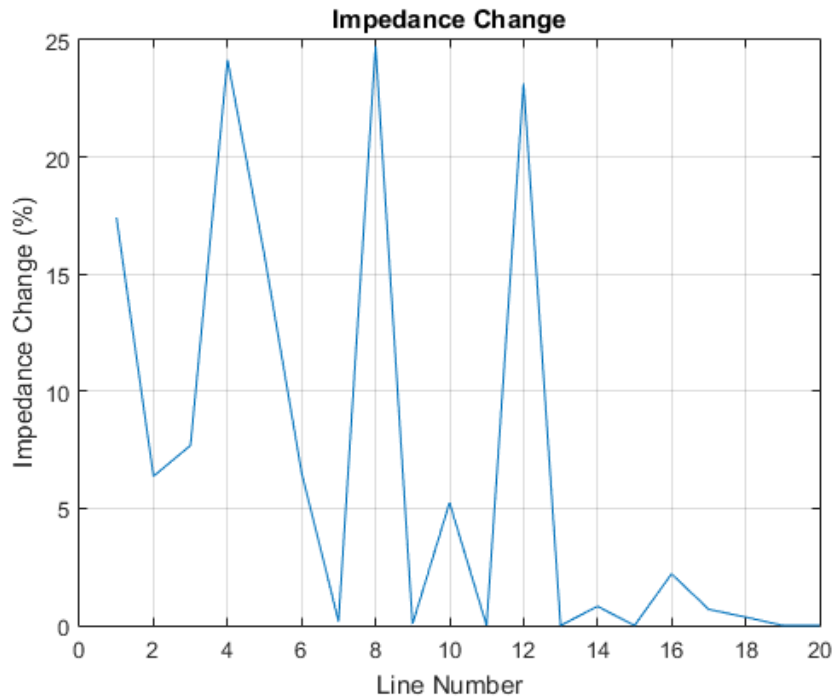
*Figure 30 IEEE 14 Bus System under 70% Load Change of Line Impedances after Loss Minimization and Power Flow Control*

### 5.1.4 14 Bus 50% load conditions

IEEE 14 bus system's bus voltage magnitudes and phase angles, load and generation information under 50% load are presented at Table 12.

*Table 12 IEEE 14 Bus Test System Busdata under 50% Load*

| Bus number | Bus voltage | | Generation | | Load | |
| --- | --- | --- | --- | --- | --- | --- |
| | Magnitude (pu) | Phase angle (degree) | Real power (MW) | Reactive power (MVAR) | Real power (MW) | Reactive power (MVAR) |
| 1 | 1.06 | 0.00 | 0.00 | 0.00 | 116.14 | -8.45 |
| 2 | 1.05 | -2.41 | 10.85 | 6.35 | 20.00 | 21.20 |
| 3 | 1.04 | -6.66 | 47.10 | 9.50 | 0.00 | 11.70 |
| 4 | 1.05 | -5.61 | 23.90 | -1.95 | 0.00 | 0.00 |

*Table 12 IEEE 14 Bus Test System Busdata under 50% Load (Continued)*

| Bus number | Bus voltage | | Generation | | Load | |
|---|---|---|---|---|---|---|
| | Magnitude (pu) | Phase angle (degree) | Real power (MW) | Reactive power (MVAR) | Real power (MW) | Reactive power (MVAR) |
| 5 | 1.05 | -4.99 | 3.80 | 0.80 | 0.00 | 0.00 |
| 6 | 1.07 | -7.81 | 5.60 | 3.75 | 0.00 | 6.11 |
| 7 | 1.06 | -7.25 | 0.00 | 0.00 | 0.00 | 0.00 |
| 8 | 1.09 | -7.25 | 0.00 | 0.00 | 0.00 | 8.68 |
| 9 | 1.06 | -7.93 | 14.75 | 8.30 | 0.00 | 0.00 |
| 10 | 1.05 | -8.05 | 4.50 | 2.90 | 0.00 | 0.00 |
| 11 | 1.06 | -7.99 | 1.75 | 0.90 | 0.00 | 0.00 |
| 12 | 1.06 | -8.22 | 3.05 | 0.80 | 0.00 | 0.00 |
| 13 | 1.06 | -8.24 | 6.75 | 2.90 | 0.00 | 0.00 |
| 14 | 1.05 | -8.56 | 7.45 | 2.50 | 0.00 | 0.00 |

First loss minimization is applied. Loss is reduced by 1.71% (0.06 MW). Figure 31 shows iterations of loss minimization algorithm. Calculation time of loss minimization is 2.33 seconds. As the system load decreases, loss minimization in MW decreases whereas calculation time for loss minimization increases.
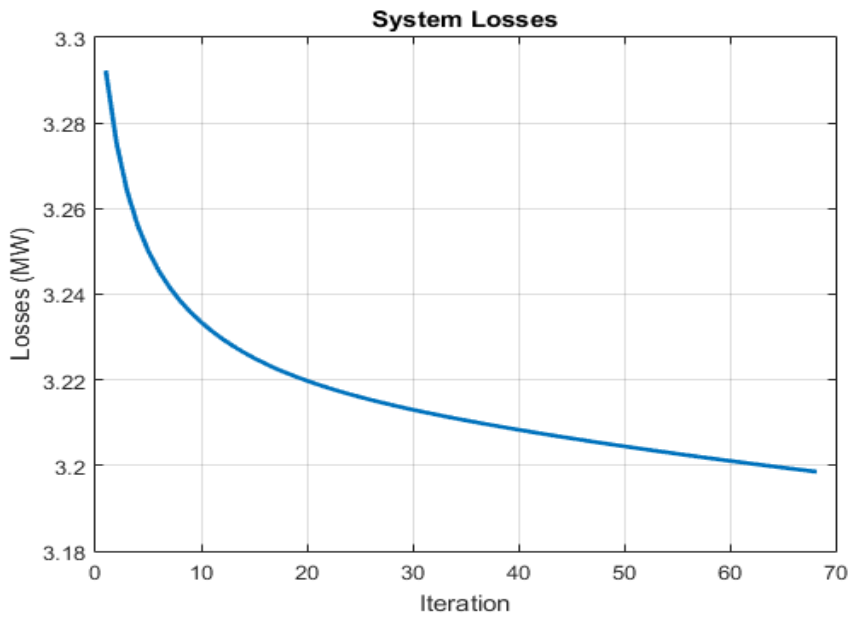
*Figure 31 IEEE 14 Bus System under 50% Load Loss Minimization*

Figures 32 and 33 show the line impedances and real power flows after loss minimization, respectively. In those figures, red lines shows the limits and green lines shows the actual values. As it can be seen from the figures below, loss minimization is achieved without any impedance and power flow limit violations.
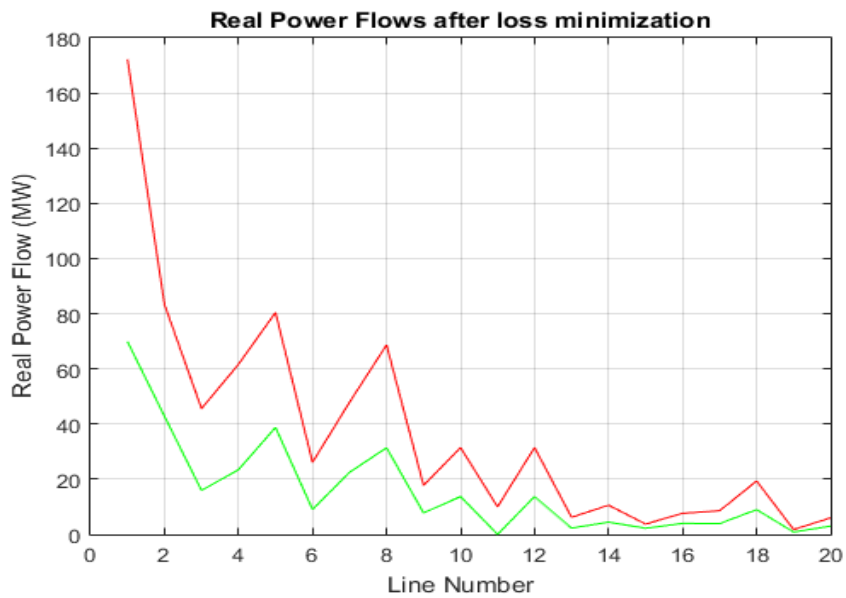


*Figure 32 IEEE 14 Bus System under 50% Load Real Power Flows after Loss Minimization*

*Figure 33 IEEE 14 Bus System under 50% Load Line Impedances and Impedance Limits after Loss Minimization*

Then power flow control is applied to lines 3 and 6 which are independently controllable. Table 13 shows the results of power flow control.

*Table 13 IEEE 14 Bus Test System under 50% Load Power Flow Control*

| Controlled lines | Initial P | Desired P | Final P |
|:---:|:---:|:---:|:---:|
| 3 | 16 | 22.4 | 22.4 |
| 6 | 9.1 | 12.8 | 12.75 |

As it can be seen from Table 13, power flow control over lines 3 and 6 is achieved simultaneously. Figures 34 and 35 show the line impedances and real power flows after loss minimization and power flow control is applied, respectively. As it can be seen from the figures below, desired controls are achieved without any impedance and power flow limit violations.
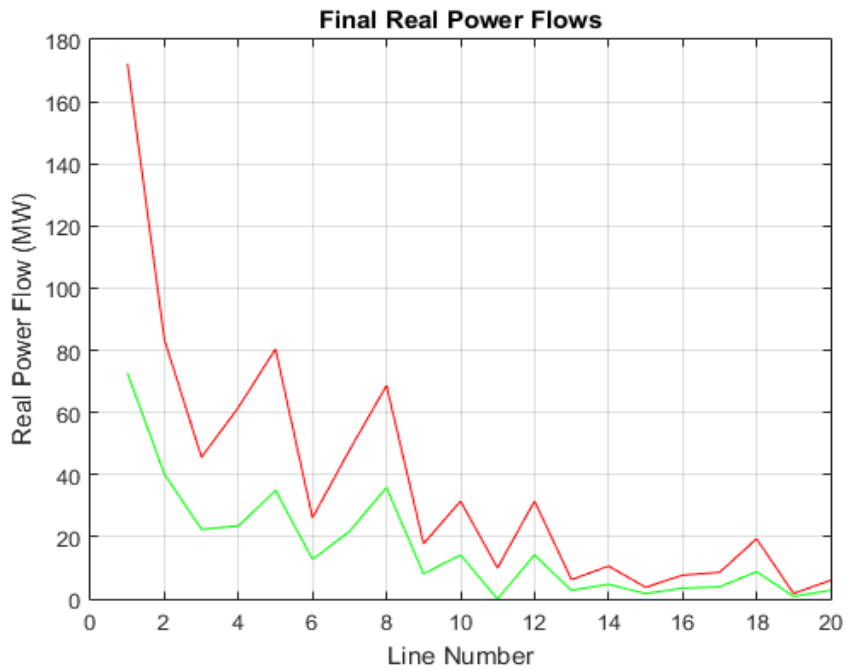
*Figure 34 IEEE 14 Bus System under 50% Load Final Real Power Flows after Loss Minimization and Power Flow Control*
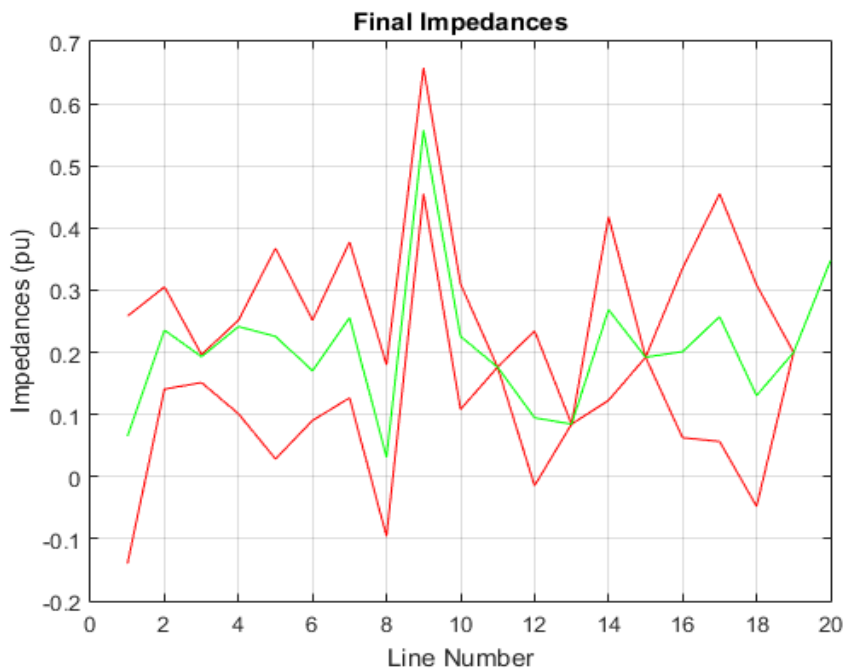


*Figure 35 IEEE 14 Bus System under 50% Load Final Line Impedances and Impedance Limits after Loss Minimization and Power Flow Control*

Figures 36 and 37 show the voltage magnitude change and total impedance change after loss minimization and power flow control, respectively. After controls are applied, voltage magnitudes are changed less than 1% and line impedance changed less than 40%. As system's load decreases, line currents decreases, and DSSC devices provide more control over line impedances. Therefore voltage magnitude change and impedance change increases.
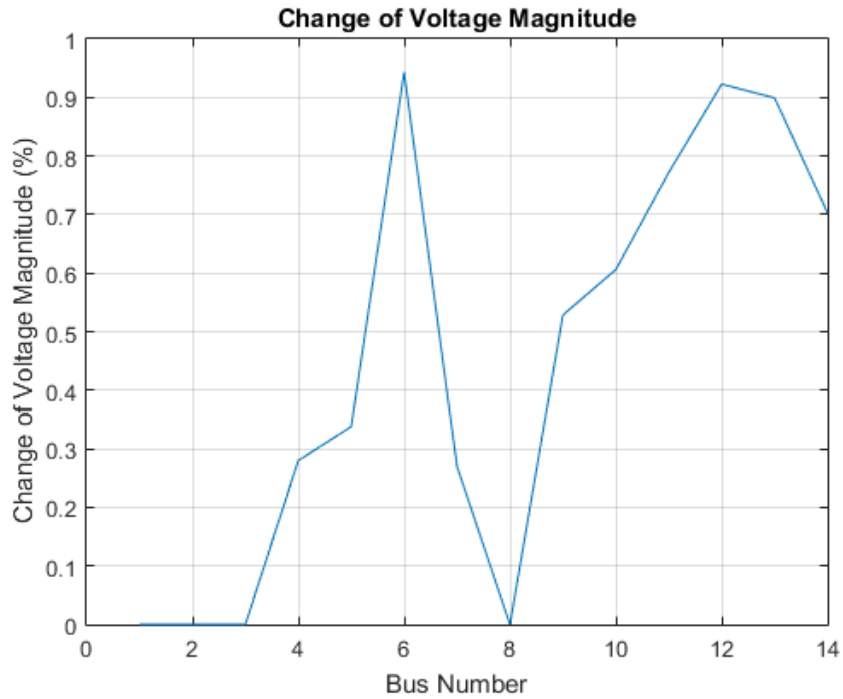


*Figure 36 IEEE 14 Bus System under 50% Load Change of Voltage Magnitudes after Loss Minimization and Power Flow Control*
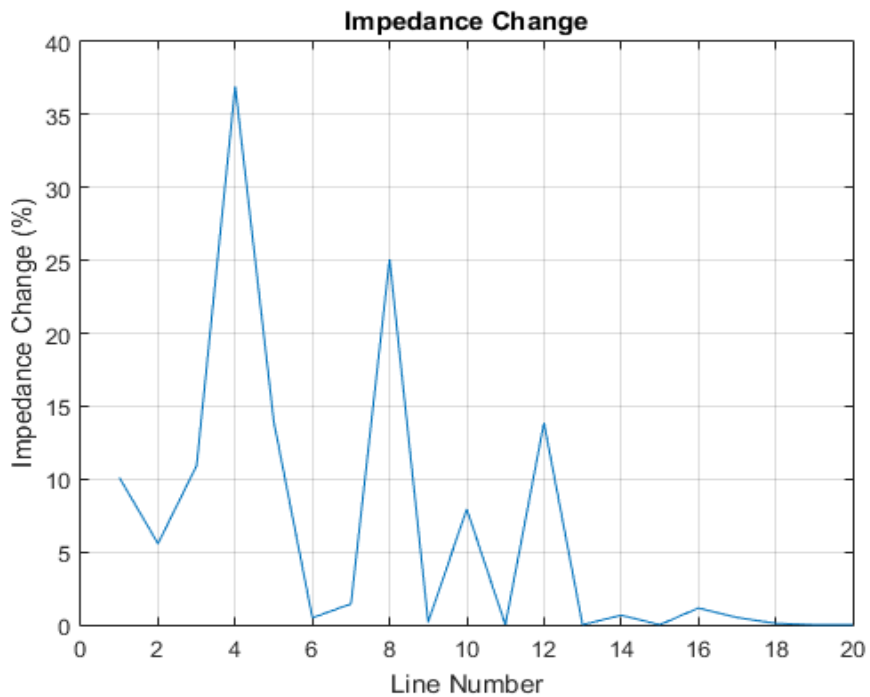
*Figure 37 IEEE 14 Bus System under 50% Load Change of Line Impedances after Loss Minimization and Power Flow Control*

## 5.2 IEEE 30 Bus Test System

Figure 38 shows the schematic diagram of IEEE 30 bus test system. System's topology information, resistance, reactance and susceptance are presented at Table 14.

IEEE 30 bus system's bus voltage magnitudes and phase angles, load and generation information under 90% load are presented at Table 15.
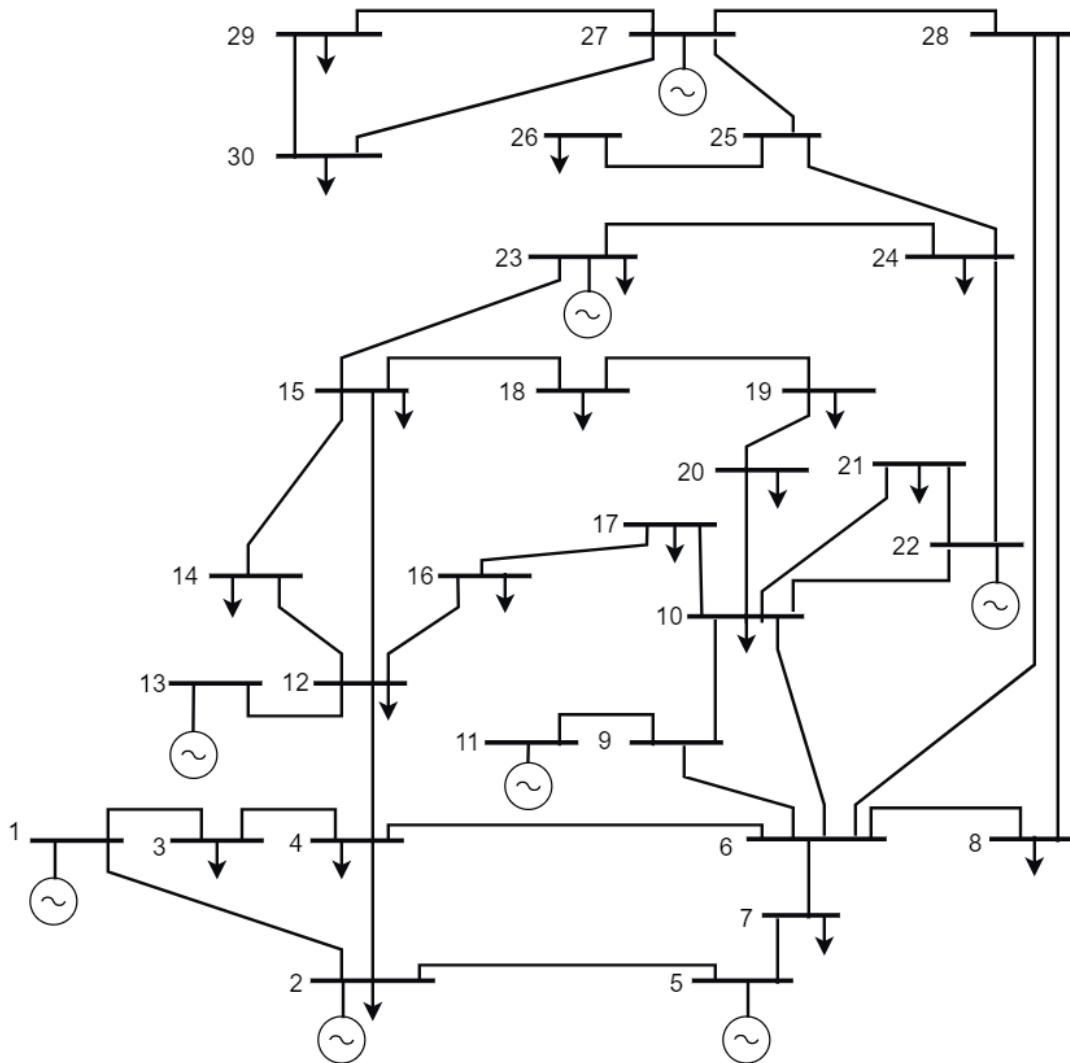
*Figure 38 IEEE 30 Bus Test System*

Impedance intervals, line limits and DSSC locations are presented in Table 16. Minimum and maximum impedance intervals, number of devices and controllable lines are determined when the system is 90% loaded. After the impedance intervals are determined, loss minimization is applied and then power flow control to lines 1 and 11. Final impedances, real power flows, loss minimization, voltage magnitude change and impedance changes are presented in the figures below. As it can be seen from Table 16, 720 DSSC devices suffice to control lines by 10% under 90% load. Lines 10, 15 and 34 are uncontrollable. 5 of the all lines are not effective on power flow, therefore DSSC devices are not placed on those lines.

*Table 14 IEEE 30 Bus Test System Line Data*

| Line No. | From bus | To bus | R (pu) | X (pu) | B (pu) |
|---|---|---|---|---|---|
| 1 | 1 | 3 | 0.05 | 0.17 | 0.04 |
| 2 | 3 | 4 | 0.01 | 0.04 | 0.01 |
| 3 | 1 | 2 | 0.02 | 0.05 | 0.05 |
| 4 | 2 | 4 | 0.06 | 0.17 | 0.04 |
| 5 | 2 | 6 | 0.06 | 0.18 | 0.04 |
| 6 | 2 | 5 | 0.05 | 0.18 | 0.04 |
| 7 | 7 | 5 | 0.05 | 0.12 | 0.02 |
| 8 | 6 | 7 | 0.03 | 0.09 | 0.02 |
| 9 | 4 | 6 | 0.01 | 0.06 | 0.01 |
| 10 | 9 | 11 | 0.00 | 0.21 | 0.00 |
| 11 | 9 | 10 | 0.00 | 0.11 | 0.00 |
| 12 | 6 | 9 | 0.00 | 0.21 | 0.00 |
| 13 | 6 | 10 | 0.00 | 0.55 | 0.00 |
| 14 | 6 | 8 | 0.01 | 0.03 | 0.01 |
| 15 | 12 | 13 | 0.00 | 0.14 | 0.00 |
| 16 | 12 | 16 | 0.09 | 0.20 | 0.00 |
| 17 | 16 | 17 | 0.05 | 0.19 | 0.00 |
| 18 | 4 | 12 | 0.00 | 0.24 | 0.00 |
| 19 | 12 | 14 | 0.12 | 0.26 | 0.00 |
| 20 | 14 | 15 | 0.22 | 0.20 | 0.00 |
| 21 | 12 | 15 | 0.07 | 0.13 | 0.00 |
| 22 | 10 | 20 | 0.09 | 0.21 | 0.00 |
| 23 | 20 | 19 | 0.03 | 0.07 | 0.00 |
| 24 | 18 | 19 | 0.06 | 0.13 | 0.00 |
| 25 | 15 | 18 | 0.11 | 0.22 | 0.00 |
| 26 | 10 | 17 | 0.03 | 0.08 | 0.00 |
| 27 | 15 | 23 | 0.10 | 0.20 | 0.00 |
| 28 | 23 | 24 | 0.13 | 0.27 | 0.00 |
| 29 | 22 | 24 | 0.12 | 0.18 | 0.00 |
| 30 | 22 | 21 | 0.01 | 0.02 | 0.01 |
| 31 | 10 | 21 | 0.03 | 0.07 | 0.00 |
| 32 | 10 | 22 | 0.07 | 0.15 | 0.00 |
| 33 | 25 | 24 | 0.19 | 0.33 | |
| 34 | 25 | 26 | 0.25 | 0.38 | |
| 35 | 27 | 25 | 0.11 | 0.21 | |
| 36 | 27 | 29 | 0.22 | 0.41 | |
| 37 | 29 | 30 | 0.24 | 0.45 | |
| 38 | 27 | 30 | 0.32 | 0.60 | |
| 39 | 28 | 27 | 0.00 | 0.39 | |
| 40 | 6 | 28 | 0.02 | 0.05 | |
| 41 | 28 | 8 | 0.06 | 0.20 | |

*Table 15 IEEE 30 Bus Test System Bus Data under 90% Load*

| Bus No | Bus voltage | | Load | | Generation | |
|---|---|---|---|---|---|---|
| | \|V\| (pu) | θ (degree) | P (MW) | Q (MVAR) | P (MW) | Q (MVAR) |
| 1 | 1.00 | 0.00 | 0.00 | 0.00 | 263.87 | -16.95 |
| 2 | 0.98 | -5.78 | 21.70 | 12.70 | 40.00 | 50.00 |
| 3 | 0.97 | -8.23 | 2.40 | 1.20 | 0.00 | 0.00 |
| 4 | 0.96 | -10.26 | 7.60 | 1.60 | 0.00 | 0.00 |
| 5 | 0.95 | -15.70 | 94.20 | 19.00 | 0.00 | 40.00 |
| 6 | 0.96 | -12.81 | 0.00 | 0.00 | 0.00 | 0.00 |
| 7 | 0.95 | -14.75 | 22.80 | 10.90 | 0.00 | 0.00 |
| 8 | 0.96 | -13.55 | 30.00 | 30.00 | 0.00 | 40.00 |
| 9 | 0.95 | -16.38 | 0.00 | 0.00 | 0.00 | 0.00 |
| 10 | 0.93 | -18.20 | 5.80 | 2.00 | 0.00 | 0.00 |
| 11 | 1.00 | -16.38 | 0.00 | 0.00 | 0.00 | 18.31 |
| 12 | 0.95 | -17.24 | 11.20 | 7.50 | 0.00 | 0.00 |
| 13 | 0.99 | -17.24 | 0.00 | 0.00 | 0.00 | 24.00 |
| 14 | 0.94 | -18.34 | 6.20 | 1.60 | 0.00 | 0.00 |
| 15 | 0.93 | -18.41 | 8.20 | 2.50 | 0.00 | 0.00 |
| 16 | 0.94 | -17.95 | 3.50 | 1.80 | 0.00 | 0.00 |
| 17 | 0.93 | -18.40 | 9.00 | 5.80 | 0.00 | 0.00 |
| 18 | 0.92 | -19.21 | 3.20 | 0.90 | 0.00 | 0.00 |
| 19 | 0.91 | -19.45 | 9.50 | 3.40 | 0.00 | 0.00 |
| 20 | 0.92 | -19.21 | 2.20 | 0.70 | 0.00 | 0.00 |
| 21 | 0.92 | -18.71 | 17.50 | 11.20 | 0.00 | 0.00 |
| 22 | 0.92 | -18.68 | 0.00 | 0.00 | 0.00 | 0.00 |
| 23 | 0.91 | -18.85 | 3.20 | 1.60 | 0.00 | 0.00 |
| 24 | 0.90 | -19.01 | 8.70 | 6.70 | 0.00 | 0.00 |
| 25 | 0.91 | -18.69 | 0.00 | 0.00 | 0.00 | 0.00 |
| 26 | 0.89 | -19.22 | 3.50 | 2.30 | 0.00 | 0.00 |
| 27 | 0.92 | -18.17 | 0.00 | 0.00 | 0.00 | 0.00 |
| 28 | 0.95 | -13.45 | 0.00 | 0.00 | 0.00 | 0.00 |
| 29 | 0.90 | -19.68 | 2.40 | 0.90 | 0.00 | 0.00 |
| 30 | 0.89 | -20.78 | 10.60 | 1.90 | 0.00 | 0.00 |

*Table 16 IEEE 30 Bus Test System Results*

| from | to | Xmin (pu) | Xmax (pu) | Plimit (MW) | Number of DSSC | Controllable |
|------|----|-----------|-----------|-------------|----------------|--------------|
| 1 | 3 | 0.15 | 0.18 | 97.3 | 42 | Yes |
| 3 | 4 | 0.02 | 0.05 | 90.8 | 36 | Yes |
| 1 | 2 | 0.03 | 0.08 | 192.6 | 306 | Yes |
| 2 | 4 | 0.17 | 0.18 | 48.1 | 6 | Yes |
| 2 | 6 | 0.17 | 0.19 | 66.7 | 18 | Yes |
| 2 | 5 | 0.17 | 0.23 | 91.3 | 84 | Yes |
| 7 | 5 | 0.12 | 0.12 | 16.2 | 0 | Yes |
| 6 | 7 | 0.07 | 0.10 | 41.8 | 12 | Yes |
| 4 | 6 | 0.00 | 0.08 | 80.3 | 87 | Yes |
| 9 | 11 | 0.21 | 0.21 | 10.0 | 0 | No |
| 9 | 10 | 0.07 | 0.15 | 30.8 | 15 | Yes |
| 6 | 9 | 0.17 | 0.24 | 30.8 | 12 | Yes |
| 6 | 10 | 0.54 | 0.57 | 17.3 | 3 | Yes |
| 6 | 8 | 0.01 | 0.08 | 32.8 | 21 | Yes |
| 12 | 13 | 0.14 | 0.14 | 10.0 | 0 | No |
| 12 | 16 | 0.20 | 0.20 | 7.6 | 3 | Yes |
| 16 | 17 | 0.19 | 0.19 | 3.6 | 0 | Yes |
| 4 | 12 | 0.23 | 0.28 | 48.0 | 21 | Yes |
| 12 | 14 | 0.24 | 0.27 | 8.7 | 3 | Yes |
| 14 | 15 | 0.20 | 0.20 | 1.8 | 0 | Yes |
| 12 | 15 | 0.09 | 0.17 | 19.4 | 6 | Yes |
| 10 | 20 | 0.20 | 0.22 | 10.0 | 3 | Yes |
| 20 | 19 | 0.06 | 0.08 | 7.5 | 3 | Yes |
| 18 | 19 | 0.13 | 0.13 | 3.0 | 0 | Yes |
| 15 | 18 | 0.21 | 0.23 | 6.6 | 3 | Yes |
| 10 | 17 | 0.08 | 0.08 | 6.3 | 0 | Yes |
| 15 | 23 | 0.20 | 0.20 | 5.2 | 3 | Yes |

Table 16 IEEE 30 Bus Test System Results (Continued)

| 23 | 24 | 0.27 | 0.27 | 1.7 | 0 | Yes |
|----|----|------|------|------|---|-----|
| 22 | 24 | 0.18 | 0.18 | 5.9 | 3 | Yes |
| 22 | 21 | 0.02 | 0.02 | 2.2 | 0 | Yes |
| 10 | 21 | 0.06 | 0.09 | 17.2 | 3 | Yes |
| 10 | 22 | 0.14 | 0.16 | 8.2 | 3 | Yes |
| 25 | 24 | 0.33 | 0.33 | 2.1 | 0 | Yes |
| 25 | 26 | 0.38 | 0.38 | 3.9 | 0 | No |
| 27 | 25 | 0.21 | 0.21 | 6.0 | 3 | Yes |
| 27 | 29 | 0.40 | 0.43 | 6.8 | 3 | Yes |
| 29 | 30 | 0.45 | 0.46 | 4.1 | 3 | Yes |
| 27 | 30 | 0.59 | 0.61 | 7.8 | 3 | Yes |
| 28 | 27 | 0.36 | 0.43 | 20.7 | 6 | Yes |
| 6 | 28 | 0.03 | 0.09 | 21.2 | 6 | Yes |
| 28 | 8 | 0.20 | 0.20 | 3.9 | 0 | Yes |

First loss minimization is applied. Loss is reduced by 0.39% (0.08 MW). Figure 39 shows iterations of loss minimization algorithm. Calculation time of loss minimization is 111 seconds. During the loss minimization process, some lines overloaded and power flow control is applied to those lines, therefore, calculation time increased.

Figures 40 and 41 show the line impedances and real power flows after loss minimization, respectively. In those figures, red lines shows the limits and green lines shows the actual values. As it can be seen from the figures below, loss minimization is achieved without any impedance and power flow limit violations despite the system is highly loaded. After loss minimization, most of the lines almost loaded up to their thermal limits.

Then power flow control is applied to lines 1 and 11 which are independently controllable. Table 17 shows the results of power flow control.
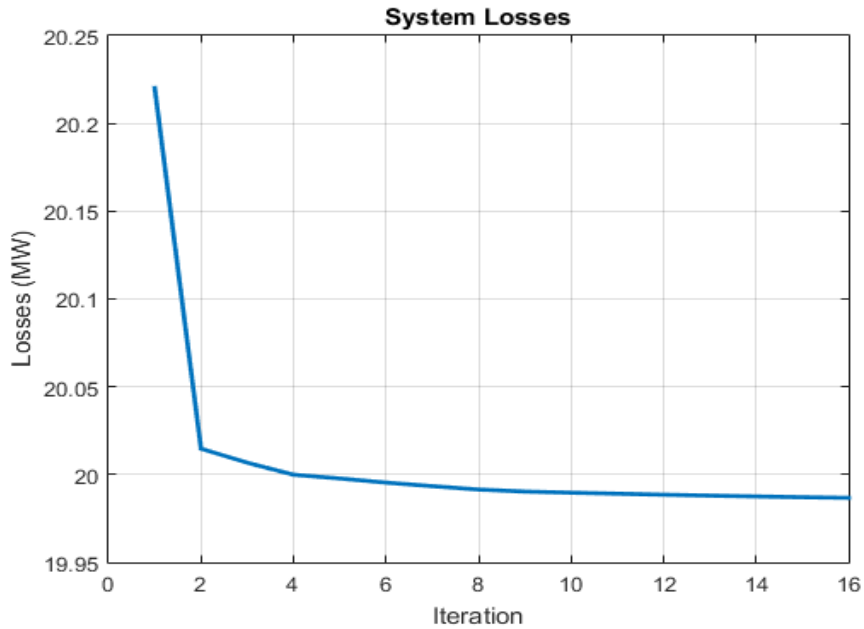


*Figure 39 IEEE 30 bus system under 90% load loss minimization*
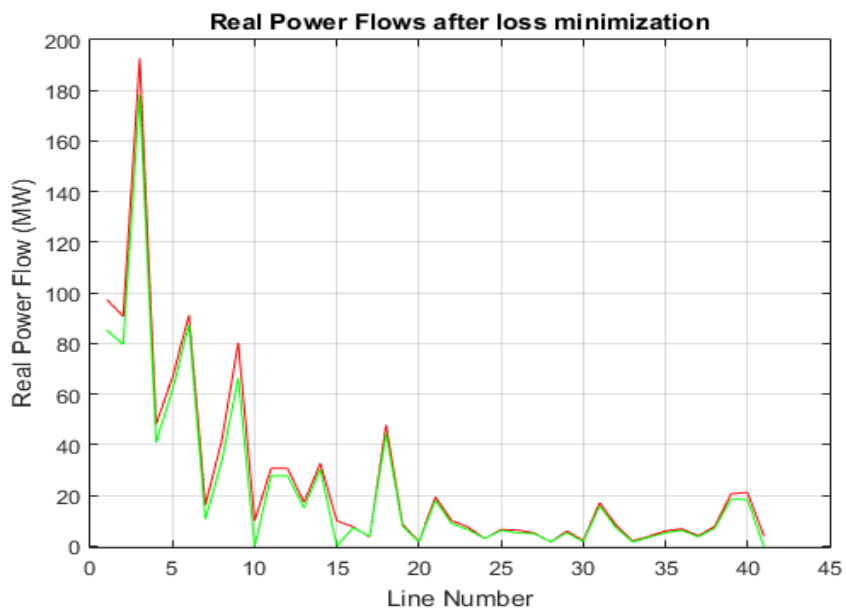


*Figure 40 IEEE 30 Bus System under 90% Load Real Power Flows after Loss Minimization*
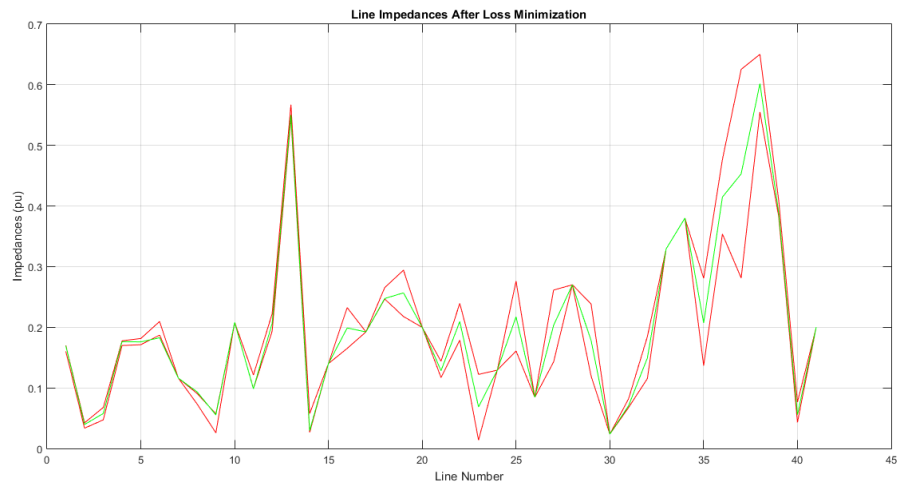
*Figure 41 IEEE 30 Bus System under 90% Load Line Impedances and Impedance Limits after Loss Minimization*

*Table 17 IEEE 30 Bus Test System under 90% Load Power Flow Control*

| Controlled lines | Initial P | Desired P | Final P |
|---|---|---|---|
| 1 | 85.34 | 81.07 | 81.08 |
| 11 | 27.77 | 26.38 | 26.46 |

As it can be seen from Table 17, power flow control over lines 1 and 11 is achieved simultaneously. Real power flows of lines 1 and 11 reduced 5% after control. Figures 42 and 43 show the line impedances and real power flows after loss minimization and power flow control is applied, respectively. As it can be seen from the figures below, desired controls are achieved without any impedance and power flow limit violations.
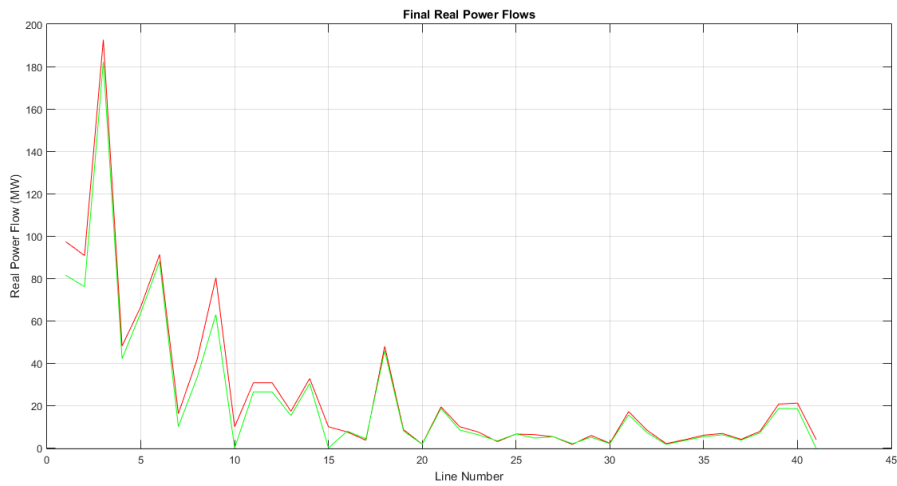
*Figure 42 IEEE 30 Bus System under 90% Load Final Real Power Flows after Loss Minimization and Power Flow Control*
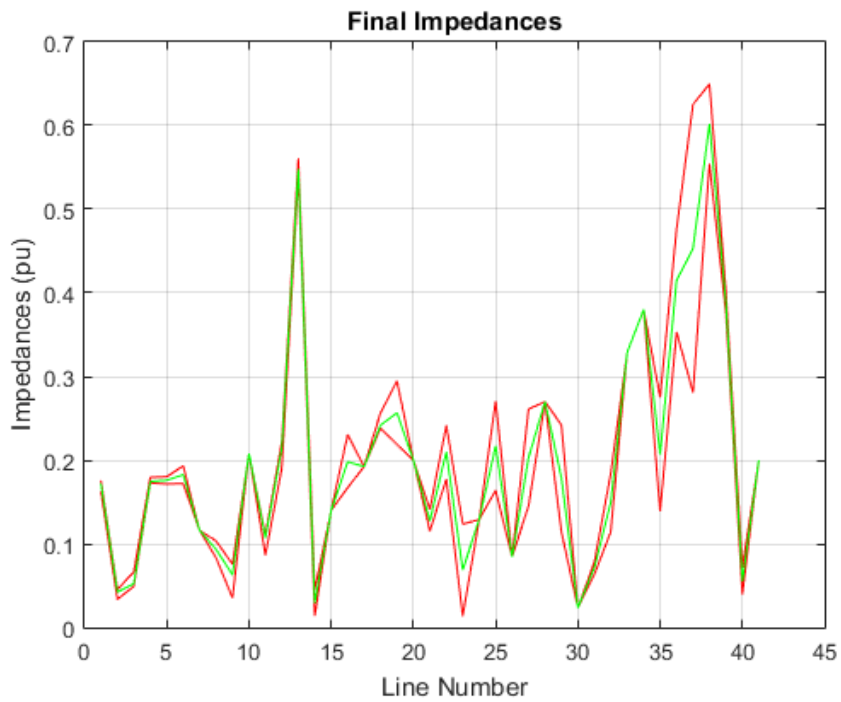


*Figure 43 IEEE 30 Bus System under 90% Load Final Line Impedances and Impedance Limits after Loss Minimization and Power Flow Control*

Figures 44 and 45 show the voltage magnitude change and total impedance change after the loss minimization and power flow control, respectively. After controls are

applied, voltage magnitudes are changed less than 1.2% and line impedance changed less than 14%.
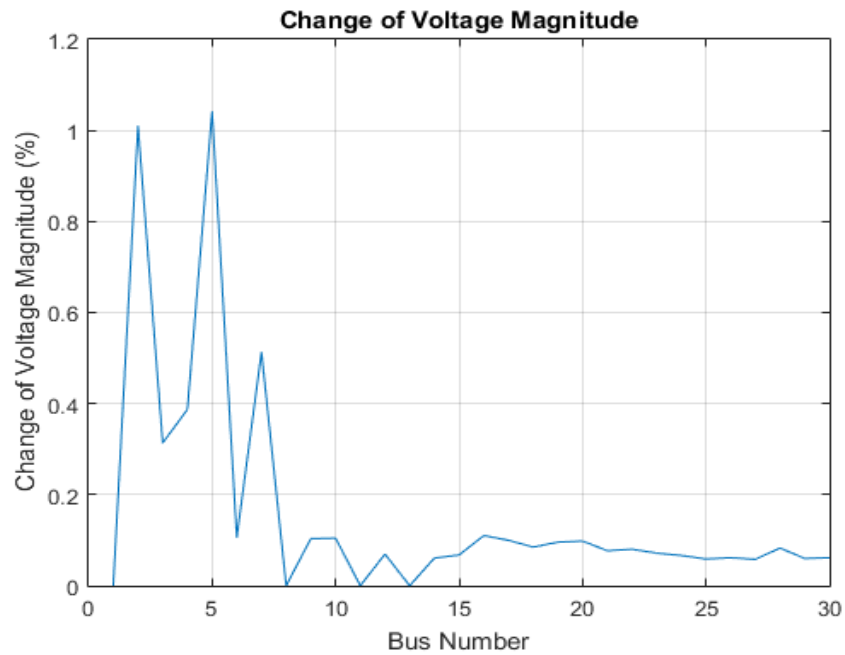


*Figure 44 IEEE 30 Bus System under 90% Load Change of Voltage Magnitude after Loss Minimization and Power Flow Control*
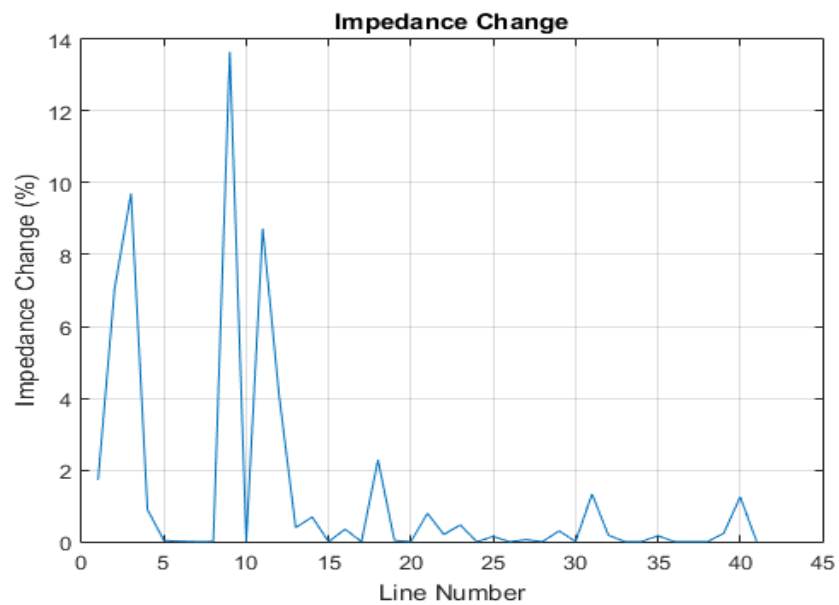


*Figure 45 IEEE 30 Bus System under 90% Load Change of Line Impedances after Loss Minimization and Power Flow Control*

## 5.3 Test Results

Table 18 and 19 presents the simulation results of IEEE 14 and 30 bus test systems. Both of them are tested under 90, 70 and 50 percent load conditions. During the tests, power flow control and loss minimization is applied. Average durations of both loss minimization and power flow control is reasonable for real time control. But, under some circumstances, those durations may be ten times more than the normal durations. It's generally due to the power flow limits or impedance limits. As it can be seen from the Table 18, average loss minimization is 0.173 MW and 0.17 MW for 14 bus and 30 bus systems, respectively. And number of DSSCs are 1644 and 720 for 14 bus and 30 bus systems, respectively. If we assume that device price is 100 dollar /kVA, electricity price is 120 dollar/MWh. Loss minimization can cover the investment cost in less than 9 and 4 years for 14 bus and 30 bus systems, respectively. As line currents reduce, number of devices to control impedances reduces, and the investment becomes more feasible. Therefore, we may infer that as the system voltage increases, necessary number of devices to control system decreases.

*Table 18 IEEE 14 and 30 Bus Test Systems Loss Minimization Results*

| System | Load | Time | loss minimization | |
| --- | --- | --- | --- | --- |
| | | | %Loss reduction | MW Loss Reduction |
| 14 bus | 90% | 1.24 | 2.24 | 0.3 |
| | 70% | 1.27 | 2.5 | 0.16 |
| | 50% | 1.27 | 1.71 | 0.06 |
| 30 bus | 90% | 111 | 0.39 | 0.08 |
| | 70% | 1.12 | 2.52 | 0.24 |
| | 50% | 2.41 | 3.94 | 0.19 |

*Table 19 IEEE 14 and 30 Bus Test Systems Power Flow Control Results*

| | | Power flow control | | | | | | | |
|---|---|---|---|---|---|---|---|---|---|
| System | Load | Time | Controlled lines | P flow | | P desired | | P final | |
| | | | | Line 1 | Line 2 | Line 1 | Line 2 | Line 1 | Line 2 |
| 14 bus | 90% | 0.48 | 3 and 6 | 33.67 | 16.91 | 31.98 | 16.07 | 31.99 | 16.11 |
| | 70% | 1.62 | 3 and 6 | 21.9 | 12.99 | 30.67 | 18.18 | 30.67 | 18.12 |
| | 50% | 2.33 | 3 and 6 | 16 | 9.1 | 22.4 | 12.8 | 22.4 | 12.75 |
| 30 bus | 90% | 4.06 | 1 and 11 | 85.34 | 27.77 | 81.07 | 26.38 | 81.08 | 26.46 |
| | 70% | 6.94 | 1 and 11 | 62.83 | 18.78 | 65.98 | 19.73 | 65.98 | 19.67 |
| | 50% | 50.79 | 1 and 11 | 46.19 | 13.14 | 62.36 | 17.74 | 61.85 | 17.06 |

## 5.4 Conclusion

When system is heavily loaded, before appling any control, effect of the control over other lines must be controlled. Coupling index is used to calculate the final power flows of uncontrolled lines. This method showed credibly results. It must be noted that, other lines final power flows should be checked if the system is heavily loaded, when system load is under 70%, any control can be applied without controlling the other lines.

As system's load decreases, line currents decreases, and DSSC devices provide more control over line impedances. Therefore voltage magnitude change and impedance change increases.

As it's proven, voltage magnitudes change less than 1% during the applied controls. Therefore, bus voltage magnitudes can't be controlled using DSSC devices. And voltage magnitudes can be eliminated from gradient of power flow control.

# CHAPTER 6

## CONCLUSION

The DSSC devices can be utilized for power flow control besides its advantages. In this study, power flow control of a power system in real time is achieved using DSSCs based on the sensitivity matrices. By controlling all the line power flows, congestion cost, which is very important in a power system can be reduced. Moreover, the system can be operated near at the minimum loss conditions. By providing 10% control, losses can be reduced at least 2% depending on the system topology and the load of system. Congestion cost minimization and loss reduction provides a great profit that can easily cover the cost of DSSC devices, such that as rated voltages of the system increase, line currents and number of DSSCs reduce, so return on investment increases.

Bus voltage magnitudes are sensitive to the line impedances but thanks to series compensation property of DSSC, bus voltages does not change significantly, such that in this study, bus voltage magnitudes change less than 0.14% during power flow control and loss minimization. Therefore, to reduce the computation time, only voltage phase angles are considered as system states while calculating the sensitivities (reduced sensitivity). Using those sensitivities decreased the computation time to solve the power flow control problem, while it increased the computation time for loss minimization solution. Therefore, reduced sensitivity is employed for power flow control, and it is mentioned that full sensitivity should be used for loss minimization.

This study assumes negligibly small reactive power flow, which is in accordance with the real life situation. Therefore, congestion is managed by controlling the real power flows. However, for ill-conditioned lines, reactive power also must be considered to control currents, such that real and reactive powers of those lines might have a negative correlation.

In this study it is aimed to control line flows in a margin of 10%. However, in a real life system, contingency analysis should be used to determine the control margin of each individual line, which may reduce the investment.

DSSC devices may facilitate the realization of a comprehensive controllable power system, such that Large-scale power flow control may finally be achievable [20].

# REFERENCES

[1]  Deepak Divan, William Brumsickle, Robert Schneider, Bill Kranz, Randal Gascoigne, Dale Bradshaw, Michael Ingram, Ian Grant, "A Distributed Static Series Compensator System for Realizing Active Power Flow Control on Existing Power Lines", IEEE Transactions on Power Delivery, vol. 22, no. 1, pp. 642-649, Jan. 2007.

[2]  W. J. Museler, President and CEO of the New York Independent System Operator (NYISO) May 22, 2003. [Online]. Available: http://www.nyiso.com/topics/articles/news_releases/2003/pa3_presentation.pdf. [Accessed 2 November 2017].

[3]  Engerati, "Comparative Performance of Smart Routers with EHV Series Capacitor," [Online]. Available: https://www.engerati.com/system/files/ssr_white_paper_by_enernex.pdf. [Accessed 8 November 2017].

[4]  ABB, "The Controllable Series Capacitor at Kanawha River," [Online]. Available: https://library.e.abb.com/public/a95f0f17f930d89dc12578fd00412422/A02-0129%20E%20HR.pdf. [Accessed 23 November 2017].

[5]  Electronics Hub, "Flexible AC Transmission System (FACTS)," [Online]. Available: https://www.electronicshub.org/flexible-ac-transmission-systemfacts/. [Accessed 29 November 2017].

[6] Progressive Media Group, "FACTS," [Online]. Available: http://static.progressivemediagroup.com/uploads/imagelibrary/nri/power/news/Alstom%20Grid.JPG. [Accessed 29 November 2017].

[7] Mereya Baby, Thilepa," Power flow control in a transmission line using D-FACTS devices", North American Power Symposium (NAPS), 2009.

[8] Power World, "D-FACTS Devices in PowerWorld Simulator," [Online]. Available: https://www.powerworld.com/files/clientconf2014/07Weber_DFACTS.pdf. [Accessed 29 November 2017].

[9] Georgia Tech, "Distributed Series Reactor," [Online]. Available: http://www.neetrac.gatech.edu/publications/140728-1856-IEEE-Presentation-Deck.pdf. [Accessed 29 November 2017].

[10] Smart Wires, "Smartvalve," [Online]. Available: https://www.smartwires.com/power-router. [Accessed 29 November 2017].

[11] Katherine M. Rogers, Thomas Overbye," Power Flow Control With Distributed Flexible AC Transmission Devices (DFACTS)", North American Power Symposium(NAPS), 2009.

[12] L. Gyugyi, C. D. Schauder, and K. K. Sen, "Static synchronous series compensator: A solid-state approach to the series compensation of transmission lines," IEEE Transactions on Power Delivery, vol. 12, no. 1, pp. 406-417, Jan. 1997.

[13] L. Gyugyi, "Dynamic compensation of AC transmission lines by solid-state synchronous voltage sources," IEEE Transactions on Power Delivery, vol. 9, no. 2, pp. 904-911, April 1994.

[14] H. Johal. "Design Considerations for Series-Connected Distributed FACTS Converters", IEEE Transactions on Industry Applications, vol. 43, no. 6, pp. 1609-1618, Nov.-Dec. 2007.

[15] Mohammed Ahmed Woday, "Contingency Analysis of Ethiopia's 230 kV Transmission Network", International Journal Of Engineering Technologies, Vol. 1, No. 4, 2015. [Online]. Available: http://dergipark.gov.tr/download/article-file/253266. [Accessed 11 November 2017].

[16] Xueqian Fu, Haoyong Chen , Xiaoming Jin, "Transient Stability of a Distribution Network with DFACTS Devices and FSWT", Power and Energy Engineering Conferance (APPEEC), Dec. 2013.

[17] A. M. A. Hamdan, A. M. Elabdalla, "Geometric Measures of Modal Controllability and Observability of Power System Models," Electric Power Systems Research, v 15, n 2, p 147-155, Oct 1988.

[18] LI Ming, WANG Yue, WANG Zhaoan, "Research on Transient Performance of D-FACTS",Electrical and Control Engineering(ICECE), Sept. 2011.

[19] S.Golshannavaz, M.Mokhtari, M.Khalilian, D.Nazarpour," Transient Stability Enhancement in Power System with Distributed Static Series Compensator (DSSC)", Electrical Engineering (ICEE), 2011.

[20] L. Gyugyi, C.D. Schauder, and K.K. Sen, "SSSC: A solid-state approach to the series compensation of transmission lines," IEEE Transactions on Power Delivery, vol. 12, no. 1, pp. 406-417, Jan. 1997.